

Environmental factors influencing benthic communities in the oxygen minimum zones on the Angolan and Namibian margins

Ulrike Hanz¹, Claudia Wienberg², Dierk Hebbeln², Gerard Duineveld¹, Marc Lavaleye¹, Katriina Juva³, Wolf-Christian Dullo³, André Freiwald⁴, Leonardo Tamborrino², Gert-Jan Reichart^{1,5}, Sascha Flögel³, Furu Mienis¹

¹*NIOZ-Royal Netherlands Institute for Sea Research and Utrecht University, Department of Ocean Systems, Texel, 1797SH, Netherlands*

²*MARUM—Center for Marine Environmental Sciences, University of Bremen, Bremen, 28359, Germany*

³*GEOMAR Helmholtz Centre for Ocean Research, Kiel, 24148, Germany*

⁴*Department for Marine Research, Senckenberg Institute, Wilhelmshaven, 26382, Germany*

⁵*Faculty of Geosciences, Earth Sciences Department, Utrecht University, Utrecht, 3512JE, Netherlands*

Correspondence to: Ulrike Hanz (ulrike.hanz@nioz.nl), +31222369466

22 Abstract

23 Thriving benthic communities were observed in the oxygen minimum zones along the southwestern
24 African margin. On the Namibian margin fossil cold-water coral mounds were overgrown by sponges and
25 bryozoans, while the Angolan margin was characterized by cold-water coral mounds covered by a living
26 coral reef. To explore why benthic communities differ in both areas, present day environmental
27 conditions were assessed, using CTD transects and bottom landers to investigate spatial and temporal
28 variations of environmental properties. Near-bottom measurements recorded low dissolved oxygen
29 concentrations on the Namibian margin of 0-0.15 ml l⁻¹ (\cong 0-9 % saturation) and on the Angolan margin
30 of 0.5-1.5 ml l⁻¹ (\cong 7-18 % saturation), which were associated with relatively high temperatures (11.8-
31 13.2 °C and 6.4-12.6 °C, respectively). Semi-diurnal barotropic tides were found to interact with the
32 margin topography producing internal waves. These tidal movements deliver water with more suitable
33 characteristics to the benthic communities from below and above the zone of low oxygen. Concurrently,
34 the delivery of high quantity and quality organic matter was observed, being an important food source
35 for the benthic fauna. On the Namibian margin organic matter originated directly from the surface
36 productive zone, whereas on the Angolan margin the geochemical signature of organic matter
37 suggested an additional mechanism of food supply. A nepheloid layer observed above the cold-water
38 corals may constitute a reservoir of organic matter, facilitating a constant supply of food particles by
39 tidal mixing. Our data suggest that the benthic fauna on the Namibian margin as well as the cold-water
40 coral communities on the Angolan margin may compensate for unfavorable conditions of low oxygen
41 levels and high temperatures with enhanced availability of food, while anoxic conditions on the
42 Namibian margin are at present a limiting factor for cold-water coral growth. This study provides an
43 example of how benthic ecosystems cope with such extreme environmental conditions since it is
44 expected that oxygen minimum zones will expand in the future due to anthropogenic activities.

45

46

47 1. Introduction

48 Cold-water corals (CWCs) form 3D structures in the deep-sea, providing important habitats for dense
49 aggregations of sessile and mobile organisms ranging from mega- to macrofauna (Henry and Roberts,
50 2007; van Soest et al., 2007) and fish (Costello et al., 2005). Consequently, CWC areas are considered as
51 deep-sea hotspots of biomass and biodiversity (Buhl-Mortensen et al., 2010; Henry and Roberts, 2017).
52 Moreover, they form hotspots for carbon cycling by transferring carbon from the water column towards
53 associated benthic organisms (Oevelen et al., 2009; White et al., 2012). Some framework-forming
54 scleractinian species, with *Lophelia pertusa* and *Madrepora oculata* being the most common species in
55 the Atlantic Ocean (Freiwald et al., 2004; White et al., 2005; Roberts et al., 2006; Cairns, 2007), are
56 capable of forming large elevated seabed structures, so called coral mounds (Wilson, 1979; Wienberg
57 and Titschack, 2017; Titschack et al., 2015; De Haas et al., 2009). These coral mounds, consisting of coral
58 debris and hemipelagic sediments, commonly reach heights between 20 and 100 m and can be several
59 kilometers in diameter. They are widely distributed along the North Atlantic margins, being mainly
60 restricted to water depths between 200-1000 m, while records of single colonies of *L. pertusa* are
61 reported from a broader depth range of 50-4000 m depth (Roberts et al., 2006; Hebbeln et al., 2014;
62 Davies et al., 2008; Mortensen et al., 2001; Freiwald et al., 2004; Freiwald, 2002; Grasmueck et al., 2006;
63 Wheeler et al., 2007).

64 A global ecological-niche factor analysis by Davies et al. (2008) and Davies and Guinotte (2011),
65 predicting suitable habitats for *L. pertusa*, showed that this species generally thrives in areas which are
66 nutrient-rich, well oxygenated and affected by relatively strong bottom water currents. Other factors
67 potentially important for proliferation of *L. pertusa* include chemical and physical properties of the
68 ambient water masses, like for example aragonite saturation state, salinity and temperature (Davies et
69 al., 2008; Dullo et al., 2008; Flögel et al., 2014; Davies and Guinotte, 2011). *L. pertusa* is most commonly
70 found at temperatures between 4-12 °C and a very wide salinity range between 32 and 38.8 (Freiwald et
71 al., 2004). The link of *L. pertusa* to particular salinity and temperature within the NE Atlantic led Dullo et
72 al. (2008) to suggest that they are restricted to a specific density envelope of sigma-theta ($\sigma\theta$) = 27.35-
73 27.65 kg m⁻³. In addition, the majority of occurrences of live *L. pertusa* comes from sites with dissolved
74 oxygen (DO) concentrations between 6-6.5 ml l⁻¹ (Davies et al., 2008), with lowest recorded oxygen
75 values being 2.1-3.2 ml l⁻¹ at CWC sites in the Gulf of Mexico (Davies et al., 2010; Schroeder, 2002;
76 Brooke and Ross, 2014) or even as low as 1-1.5 ml l⁻¹ off Mauritania where CWC mounds are in a
77 dormant stage showing only scarce living coral occurrences today (Wienberg et al., 2018; Ramos et al.,
78 2017). Dissolved oxygen levels hence seem to affect the formation of CWC structures as was also shown

79 by Holocene records obtained from the Mediterranean Sea, which revealed periods of reef demise and
80 growth in conjunction with hypoxia (with 2 ml l^{-1} seemingly forming a threshold value for active coral
81 growth; Fink et al., 2012).

82 Another essential constraint for CWC growth and therefore mound development in the deep-sea is food
83 supply. *L. pertusa* is an opportunistic feeder, exploiting a wide variety of different food sources,
84 including phytodetritus, phytoplankton, mesozooplankton, bacteria and dissolved organic matter
85 (Kiriakoulakis et al., 2005; Dodds et al., 2009; Gori et al., 2014; Mueller et al., 2014; Duineveld et al.,
86 2007). Not only quantity but also quality of food particles is of crucial importance for the uptake
87 efficiency as well as ecosystem functioning of CWCs (Ruhl, 2008; Mueller et al., 2014). Transport of
88 surface organic matter towards CWC sites at intermediate water depths has been found to involve
89 either active swimming (zooplankton), passive sinking, advection, local downwelling, and internal waves
90 and associated mixing processes resulting from interactions with topography (Davies et al., 2009; van
91 Haren et al., 2014; Thiem et al., 2006; White et al., 2005; Mienis et al., 2009; Frederiksen et al., 1992).
92 With worldwide efforts to map CWC communities, *L. pertusa* was also found under conditions which are
93 environmentally stressful or extreme in the sense of the global limits defined by Davies et al. (2008) and
94 Davies and Guinotte (2011). Examples are the warm and salty waters of the Mediterranean and the high
95 bottom water temperatures along the US coast (Cape Lookout; (Freiwald et al., 2009; Mienis et al.,
96 2014; Taviani et al., 2005). Environmental stress generally increases energy needs for organisms to
97 recover and maintain optimal functioning, which accordingly increases their food demand (Sokolova et
98 al., 2012).

99 For the SW African margin one of the few records of living CWC comes from the Angolan margin (at 7° S ;
100 (Le Guilloux et al., 2009), which raises the question whether environmental factors limit CWC growth
101 due to the presence of an Oxygen Minimum Zone (OMZ; see Karstensen et al. 2008), or whether this is
102 related to a lack of data. Hydroacoustic campaigns revealed extended areas off Angola and Namibia with
103 structures that morphologically resemble coral mound structures known from the NE Atlantic (M76-3,
104 MSM20-1; Geissler et al., 2013; Zabel et al., 2012). Therefore two of such mound areas on the margins
105 off Namibia and Angola were visited during the RV *Meteor* cruise M122 'ANNA' (ANGola/NAMibia) in
106 January 2016 (Hebbeln et al., 2017). During this cruise fossil CWC mound structures were found near
107 Namibia, while flourishing CWC reef-covered mound structures were observed on the Angolan margin.
108 The aim of the present study was to assess present-day environmental conditions at the southwestern
109 African margin to explore why CWCs thrive on the Angolan margin and are absent on the Namibian

110 margin. Key parameters influencing CWCs, hydrographic parameters as well as chemical properties of
111 the water column were measured to characterize the difference in environmental conditions and food
112 supply. These data are used to improve understanding of the potential fate of CWC mounds in a
113 changing ocean.

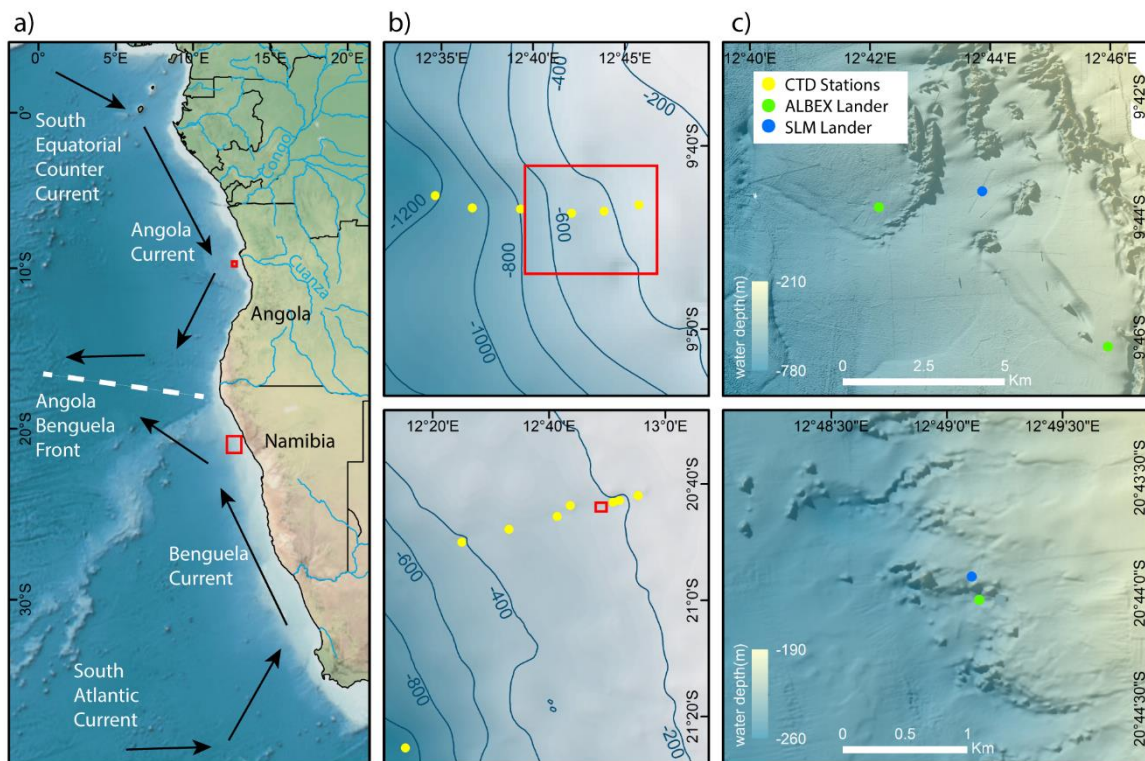
114 2. Material and Methods

115 2.1 *Setting*

116 2.1.1 *Oceanographic setting*

117 The SW African margin is one of the four major eastern boundary regions in the world and is
118 characterized by upwelling of nutrient-rich cold waters (Shannon and Nelson, 1996). The availability of
119 nutrients triggers a high primary production, making it one of the most productive marine areas
120 worldwide with an estimated production of 0.37 Gt C/yr (Carr and Kearns, 2003). Remineralization of
121 high fluxes of organic particles settling through the water column results in severe mid-depth oxygen
122 depletion and an intense OMZ over large areas along the SW African margin (Chapman and Shannon,
123 1985). The extension of the OMZ is highly dynamic being controlled by upwelling intensity, which
124 depends on the prevailing winds and two current systems along the SW African margin, i.e. the Benguela
125 and the Angola currents (Kostianoy and Lutjeharms, 1999; Chapman and Shannon, 1987; Fig. 1). The
126 Benguela Current originates from the South Atlantic Current, which mixes with water from the Indian
127 Ocean at the southern tip of Africa (Poole and Tomczak, 1999; Mohrholz et al., 2008; Rae, 2005) and
128 introduces relatively cold and oxygen-rich Eastern South Atlantic Central Water (ESACW; Poole and
129 Tomczak 1999) to the SW African margin (Mohrholz et al., 2014). The Angola Current originates from the
130 South Equatorial Counter Current and introduces warmer, nutrient-poor and less oxygenated South
131 Atlantic Central Water (SACW; Poole and Tomczak (1999) to the continental margin (Fig. 1a). SACW is
132 defined by a linear relationship between temperature and salinity in a T-S plot (Shannon et al., 1987).
133 While the SACW flows along the continental margin the oxygen concentration is decreasing
134 continuously due to remineralisation processes of organic matter on the SW African shelf (Mohrholz et
135 al., 2008). Both currents converge at around 14-16 °S, resulting in the Angola-Benguela Front
136 (Lutjeharms and Stockton, 1987). In austral summer, the Angola-Benguela Front can move southward to
137 23 °S (Shannon et al., 1986), thus increasing the influence of the SACW along the Namibian coast (Junker
138 et al., 2017; Chapman and Shannon, 1987), contributing to the pronounced OMZ due to its low initial
139 oxygen concentration (Poole and Tomczak, 1999). ESACW is the dominant water mass at the Namibian
140 margin during the main upwelling season in austral winter, expanding from the oceanic zone about 350

141 km towards the coast. (Mohrholz et al., 2014). The surface water mass at the Namibian margin is a
 142 mixture of sun-warmed upwelled water and water of the Agulhas Current, which mixes in complex
 143 eddies and filaments and is called South Atlantic Subtropical Surface Water (SASSW) (Hutchings et al.,
 144 2009). At the Angolan margin the surface water is additionally influenced by water from the Cuanza and
 145 Congo rivers (Kopte et al., 2017, Fig. 1). Antarctic Intermediate Water (AAIW) is situated in deeper areas
 146 at the African continental margin and can be identified as the freshest water mass around 700-800 m
 147 depth (Shannon and Nelson, 1996).



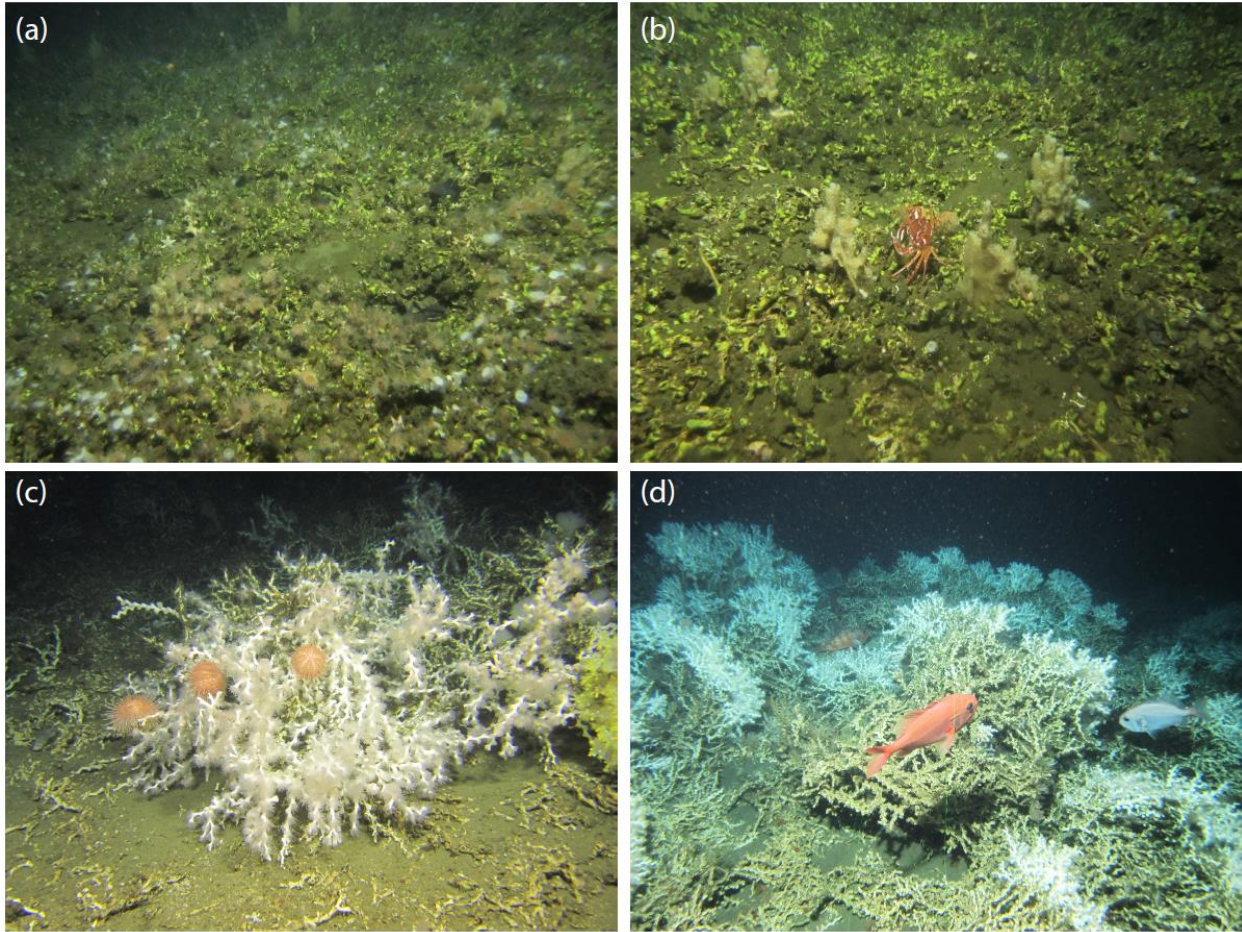
148
 149 **Figure 1** (a) Overview map showing the research areas off Angola and Namibia (red squares) and main features of the surface
 150 water circulation (arrows) and frontal zone (dashed line) as well as the two main rivers discharging at the Angolan margin.
 151 Detailed bathymetry maps of the Angolan (upper maps) and Namibian margins (lower maps) showing the position of (b) CTD
 152 transects (note the deep CTD cast down to 1000 m water depth conducted off Namibia) and (c) bottom lander deployments
 153 (red squares shown in (b) indicate the cutouts displayed in (c)).

154 2.1.2. Coral mounds along the Angolan and Namibian margins

155 During RV *Meteor* cruise M122 in 2016, over 2000 coral mounds were observed between 160-260 m
 156 water depth on the Namibian shelf (Hebbeln et al., 2017). All mounds were densely covered with coral

157 rubble and dead coral framework, while no living corals were observed in the study area (Hebbeln et al.,
158 2017; Figs. 2a, b). Few species were locally very abundant, viz. a yellow cheilostome bryozoan which was
159 the most common species, and five sponge species. The bryozoans were encrusting the coral rubble,
160 whereas some sponge species reached heights of up to 30 cm (Fig. 2a, b). The remaining community
161 consisted of an impoverished fauna overgrowing *L. pertusa* debris. Commonly found sessile organism
162 were actinarians, zoanthids, hydroids, some thin encrusting sponges, serpulids and sabellid polychaetes.
163 The mobile fauna comprised asteroids, ophiuroids, two shrimp species, amphipods, cumaceans and
164 holothurians. Locally high abundances of *Suffogobius bibarbatus*, a fish that is known to be adapted to
165 hypoxic conditions, were observed in cavities in the coral framework (Hebbeln, 2017). Dead corals
166 collected from the surface of various Namibian mounds date back to about 5 ka BP, pointing to a
167 simultaneous demise of these mounds during the mid-Holocene (Tamborrino et al., accepted).

168 On the Angolan margin CWC structures varied from individual mounds to long ridges. Some mounds
169 reached heights of more than 100 m above the seafloor. At shallow depths (~250 m) some isolated
170 smaller mounds were also present (Hebbeln et al. 2017). All mounds showed a thriving CWC cover,
171 which was dominated by *L. pertusa* (estimated 99% relative abundance), along with some *M. oculata*
172 and solitary corals. Mounds with a flourishing coral cover were mainly situated at water depths between
173 330-470 m, whereas single colonies were found over a broader depth range between 250-500 m (Figs.
174 2c, d; Hebbeln et al., 2017). Additionally, large aggregations of hexactinellid sponges (*Aphrocallistes*,
175 *Sympagella*) were observed. First estimates for coral ages obtained from a gravity core collected at one
176 of the Angolan coral mounds revealed continuous coral mound formation during the last 34 ka until
177 today (Wefing et al., 2017).



178

179 **Figure 2** ROV images (copyright MARUM ROV SQUID, Bremen, Germany) showing the surface coverage of cold-water coral
 180 mounds discovered off Namibia (a, b) and Angola (c, d). Images were recorded and briefly described for their faunal
 181 composition during RV *Meteor* cruise M122 "ANNA" (see Hebbeln et al. 2017). (a) Sylvester mound, 225 m water depth. Dead
 182 coral framework entirely consisting of *L. pertusa*. The framework is intensely colonized by the yellow bryozoan *Metropriella* sp.,
 183 zoanthids, actinarians and sponges. Vagile fauna consists of asteroids and gobiid fishes (*Sufflogobius bibarbatus*) that hide in
 184 hollows in the coral framework. (b) Sylvester mound, 238 m water depth. Dense coral rubble (*L. pertusa*) heavily overgrown by
 185 *Metropriella* sp. and sponges. Note the decapod crab *Macropipus australis* (center of the image). (c) Valentine mound, 238 m
 186 water depth. Live *L. pertusa* colony being grazed by echinoids. Note the sponge *Aphrocallistes* sp. with its actinarian symbionts
 187 (right side of the image). (d) Buffalo mound, 345 m water depth. Living CWC reef observed on top of an Angolan coral mound.
 188 Many fishes are present around the reef (*Helicolenus dactylopterus*, *Gephyroberyx darwinii*).

189 2.2 Methodology

190 During RV *Meteor* expedition M122 in January 2016, two CTD transects and three short-term bottom
 191 lander deployments (Table 1, Fig. 1) were carried out to measure environmental conditions influencing
 192 benthic habitats. In addition, weather data were continuously recorded by the RV *Meteor* weather
 193 station, providing real-time information on local wind speed and wind direction.

194 *2.2.1 Lander deployments*

195 Sites for deployment of the NIOZ designed lander (ALBEX) were selected based on multibeam
196 bathymetric data. On the Namibian margin the bottom lander was deployed on top of a mound
197 structure (water depth 220 m). Off Angola the lander was deployed in the relatively shallow part of the
198 mound zone at 340 m water depth and in the deeper part at 530 m (Fig. 1, Table 1). Additionally, a
199 GEOMAR Satellite Lander Module (SLM) was deployed off-mound in 230 m depth at the Namibian
200 margin and at 430 m depth at the Angolan margin (Fig. 1, Table 1). The lander was equipped with an
201 ARO-USB oxygen sensor (JFE-Advantech™), a combined OBS-fluorometer (Wetlabs™) and an Aquadopp
202 (Nortek™) profiling current meter. The lander was furthermore equipped with a Technicap PPS4/3
203 sediment trap with 12 bottles (allowing daily samples) and a McLane particle pump (24 filter units for
204 each 7.5 L of seawater, two hour interval) to sample particulate organic matter in the near-bottom
205 water (40 cm above bottom).

206 The SLM was equipped with a 600 kHz ADCP Workhorse Sentinel 600 from RDI, a CTD (SBE SBE16V2™), a
207 combined fluorescence and turbidity sensor (WET Labs ECO-AFL/FL), a dissolved oxygen sensor (SBE™)
208 and a pH sensor (SBE™) (Hebbeln et al., 2017). From the SLM only pH measurements are used here,
209 complementing the data from the NIOZ lander.

210 *2.2.2 CTD transects*

211 Vertical profiles of hydrographic parameters in the water column, viz. temperature, conductivity, oxygen
212 and turbidity, were obtained using a Seabird CTD/Rosette system (Seabird SBE 9 plus). The additional
213 sensors on the CTD were a dissolved oxygen sensor (SBE 43 membrane-type DO Sensor) and a combined
214 fluorescence and turbidity sensor (WET Labs ECO-AFL/FL). The CTD was combined with a rosette water
215 sampler consisting of 24 Niskin® water sampling bottles (10 L). CTD casts were carried out along two
216 downslope CTD transects (Fig. 1). Owing to technical problems turbidity data were only collected on the
217 Angolan slope.

218 *2.2.3 Hydrographic data processing*

219 The CTD data were processed using the processing software Seabird data SBE 11plus V 5.2 and were
220 visualized using the program Ocean Data View (Schlitzer (2011); Version 4.7.8).

221 Hydrographic data recorded by the landers were analyzed and plotted using the program R (R Core
222 Team, 2017). Data from the different instruments (temperature, turbidity, current speed, oxygen
223 concentration, fluorescence) were averaged over a period of 1.5 h to remove shorter term trends and
224 occasional spikes. Correlations between variables were assessed by Spearman's rank correlation tests.

225 *2.2.4 Suspended particulate matter*

226 Near-bottom suspended particulate organic matter (SPOM) was sampled by means of a phytoplankton
227 sampler (McLane PPS) mounted on the ALBEX lander. The PPS was fitted with 24 GF/F filters (47 mm
228 Whatman™ GF/F filters pre-combusted at 450 °C). A maximum of 7.5 L was pumped over each filter
229 during a 2h period yielding a time series of near bottom SPOM supply and its variability over a period of
230 48 hours.

231 *C/N analysis and isotope measurements*

232 Filters from the phytoplankton sampler were freeze-dried before further analysis. Half of each filter was
233 used for phytopigment analysis and a ¼ section of each filter was used for analyzing organic carbon,
234 nitrogen, and their stable isotope ratios. The filters used for carbon analysis were decarbonized by vapor
235 of concentrated hydrochloric acid (2 M HCl supra) prior to analyses. Filters were transferred into pressed
236 tin capsules (12x5 mm, Elemental Microanalysis) and $\delta^{15}\text{N}$, $\delta^{13}\text{C}$ and total weight percent of organic
237 carbon and nitrogen were analyzed by a Delta V Advantage isotope ratio MS coupled on line to an
238 Elemental Analyzer (Flash 2000 EA-IRMS) by a ConFlo IV (Thermo Fisher Scientific Inc.). The reference gas
239 was purified atmospheric N_2 . As standards for $\delta^{13}\text{C}$ benzoic acid and acetanilide were used, for $\delta^{15}\text{N}$
240 acetanilide, urea and casein was used. For $\delta^{13}\text{C}$ analysis a high signal method was used including a 70%
241 dilution. Values are reported relative to v-pdb and the atmosphere respectively. Precision and accuracy
242 based on replicate analyses and comparison with international standards for $\delta^{13}\text{C}$ and $\delta^{15}\text{N}$ was ± 0.15
243 ‰. The C/N ratio is based on the weight ratios between TOC and N.

244 *Phytopigments*

245 Phytopigments were measured by reverse-phase high-performance liquid chromatography (RP-HPLC,
246 Waters Acquity UPLC) with a gradient based on the method published by (Kraay et al., 1992). For each
247 sample half of a GF/F filter was used and freeze-dried before extraction. Pigments were extracted using
248 95% methanol and sonification. All steps were performed in a dark and cooled environment. Pigments
249 were identified by means of their absorption spectrum, fluorescence and the elution time. Identification
250 and quantification took place as described by Tahey et al. (1994). The absorbance peak areas of
251 chlorophyll- α were converted into concentrations using conversion factors determined with a certified
252 standard. The $\Sigma\text{Phaeopigment}/\text{Chlorophyll-}\alpha$ ratio gives an indication of the degradation status of the
253 organic material, since phaeopigments form as a result of bacterial or autolytic cell lysis and grazing
254 activity (Welschmeyer and Lorenzen, 1985).

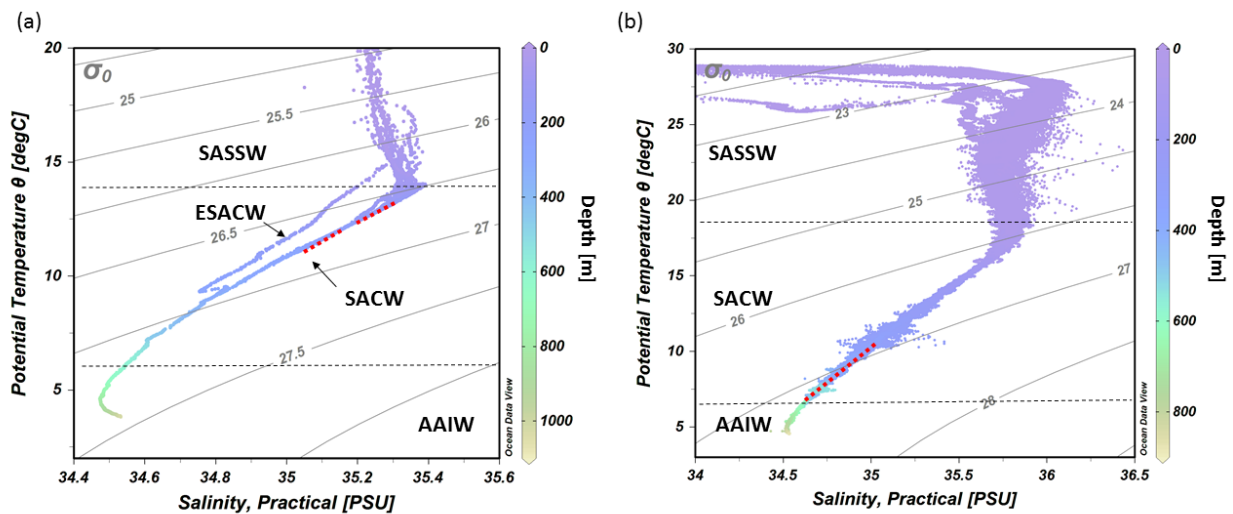
255 2.2.5 Tidal analysis
 256 The barotropic (due to the sea level and pressure change) and baroclinic (internal ‘free waves’
 257 propagating along the pycnoclines) tidal signals obtained by the Aquadopp (Nortek™) profiling current
 258 meter were analyzed from the bottom pressure and from the horizontal flow components recorded 6 m
 259 above the sea floor, using the harmonic analysis toolbox t_tide (Pawlowicz et al., 2002). The data mean
 260 and trends were subtracted from the data before analysis.

261 3. Results

262 3.1 Water column properties

263 3.1.1 Namibian margin

264 The hydrographic data obtained by CTD measurements along a downslope transect from the surface to
 265 1000 m water depth revealed distinct changes in temperature and salinity throughout the water
 266 column. These are ascribed to the different water masses in the study area (Fig. 3a). In the upper 85 m
 267 of the water column, temperatures were above 14 °C and salinities > 35.2, which corresponds to South
 268 Atlantic Subtropical Surface Water (SASSW). SACW was situated underneath the SASSW and reaches
 269 down to about 700 m, characterized by a temperature from 14-7 °C and a salinity from 35.4-34.5 (Fig.
 270 3a). A deep CTD cast about 130 km from the coastline recorded a water mass with the signature of
 271 ESACW, having a lower temperature (Δ 1.3 °C) and lower salinity (Δ 0.2) than SACW (in 200 m depth, not
 272 included in CTD transects of Fig. 4). Underneath these two central water masses Antarctic Intermediate
 273 Water (AAIW) was found with a temperature <7 °C.



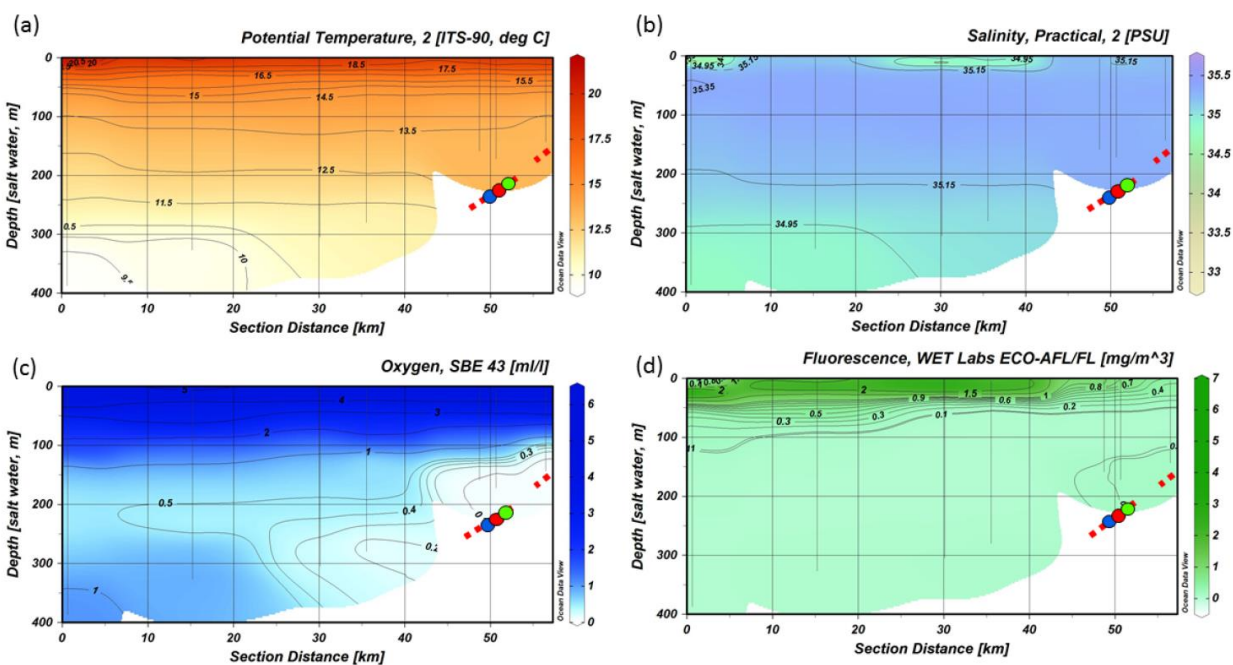
274

275 **Figure 3** TS-diagrams showing the different water masses being present at the (a) Namibian and (b) Angolan margins: South
 276 Atlantic Subtropical Surface Water (SASSW), South Atlantic Central Water (SACW) and Eastern South Atlantic Central water

277 (ESACW), Antarctic Intermediate Water (AAIW) (data plotted using Ocean Data View v.4.7.8; <http://odv.awi.de>; Schlitzer, 2011).
278 Red dotted line indicates the depth range of cold-water coral mound occurrence.

279 The CTD transect showed decreasing DO (dissolved oxygen) concentration from the surface (6 ml l^{-1})
280 towards a minimum in 150-200 m depth (0 ml l^{-1}). Lowest values for DO concentrations were found on
281 the continental margin between 100-335 m water depth. The DO concentrations in this pronounced
282 OMZ ranged from $<1 \text{ ml l}^{-1}$ down to 0 ml l^{-1} ($\pm 9-0 \%$ saturation, respectively). The zone of low DO
283 concentrations ($<1 \text{ ml l}^{-1}$) stretched horizontally over the complete transect from about 50 to at least
284 100 km offshore (Fig. 4c). The upper boundary of the OMZ was relatively sharp compared to its lower
285 limits and corresponded with the border between SASSW at the surface and SACW below.

286 Within the OMZ, a small increase in fluorescence (0.2 mg m^{-3}) was recorded, whereas fluorescence was
287 otherwise not traceable below the surface layer (Fig. 4d). Within the surface layer highest surface
288 fluorescence ($>2 \text{ mg m}^{-3}$) was found $\sim 40 \text{ km}$ offshore. Above the center of the OMZ fluorescence
289 reached only 0.4 mg m^{-3} .

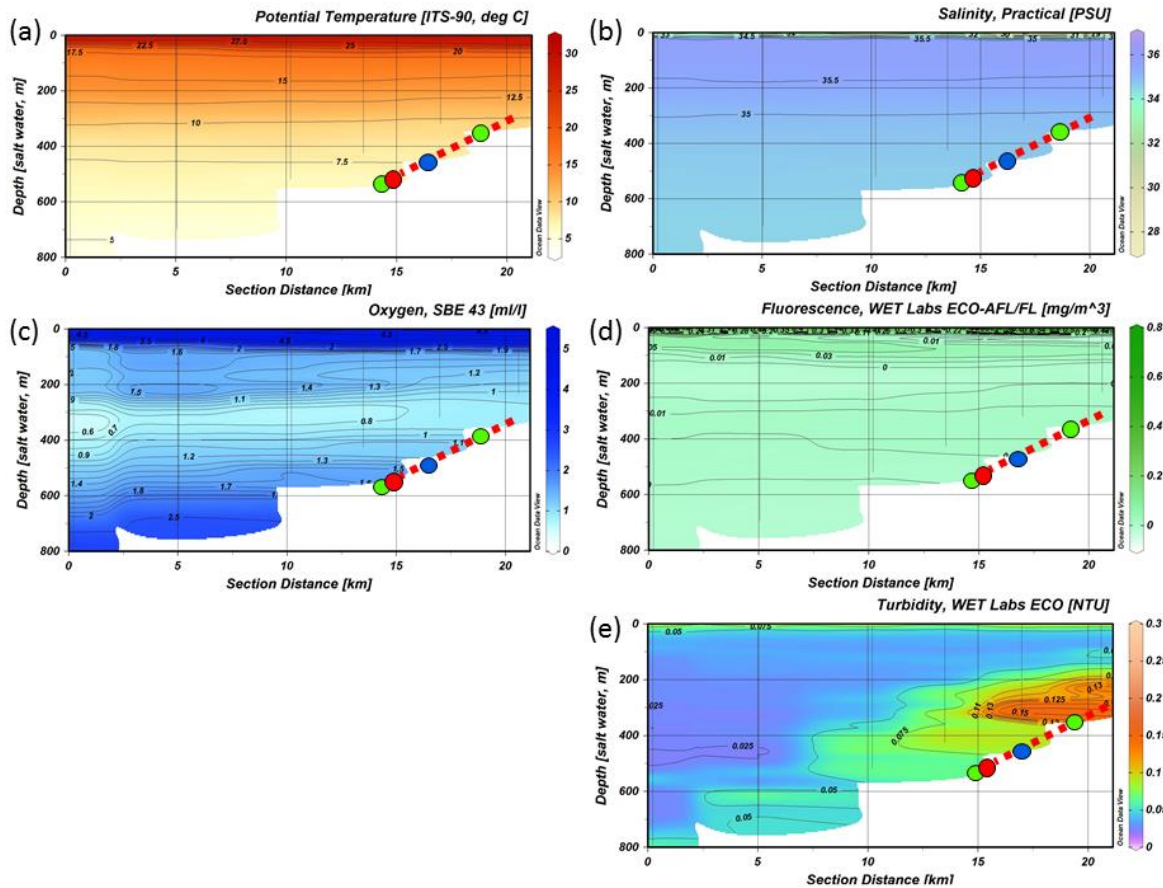


290
291 **Figure 4** CTD transect across the Namibian margin (see Fig. 1b for location). Data are presented for: (a) potential temperature
292 ($^{\circ}\text{C}$), (b) salinity (PSU), (c) dissolved oxygen concentrations (ml l^{-1}), note the pronounced oxygen minimum zone (OMZ) between
293 100-335 m water depth, and (d) fluorescence (mg m^{-3}) (data plotted using Ocean Data View v.4.7.8; <http://odv.awi.de>; Schlitzer,
294 2011). The occurrence of fossil CWC mounds is indicated by a red dashed line, colored dots indicate bottom lander
295 deployments.

296 *3.1.2 Angolan margin*

297 The hydrographic data obtained by CTD measurements along a downslope transect from the surface to
298 800 m water depth revealed distinct changes in temperature and salinity throughout the water column,
299 related to four different water masses. At the surface a distinct shallow layer (>20 m) with a distinctly
300 lower salinity (27.3-35.5) and higher temperature (29.5-27 °C, Fig. 3b) was observed. Below the surface
301 layer, SASSW was found down to a depth of 70 m, characterized by a higher salinity (35.8). SACW was
302 observed between 70-600 m, showing the expected linear relationship between temperature and
303 salinity. Temperature and salinity decreased from 17.5 °C/35.8 to 7° C/34.6. At 700 m depth AAIW was
304 recorded, characterized by a low salinity (<34.4) and temperature (<7 °C, Fig. 3b).

305 The CTD transect showed a sharp decrease in the DO concentrations underneath the SASSW from 5 to
306 <2 ml l⁻¹ (Fig. 5). DO concentrations decreased further to a minimum of 0.6 ml l⁻¹ at 350 m and then
307 increased to >3 ml l⁻¹ at 800 m depth. Lowest DO concentrations were not found at the slope but 70 km
308 offshore in the center of the zone of reduced DO concentrations between 200-450 m water depth (<1
309 ml l⁻¹). Compared to the Namibian margin (see Fig. 4), the hypoxic layer was situated further offshore,
310 slightly deeper and overall DO concentrations were higher (compare Fig. 4c). Also, the boundaries of the
311 hypoxic zone were not as sharp. Fluorescence near the sea surface was generally low (around 0.2 with
312 small maxima of 0.78 mg m⁻³) and not detectable deeper than 150 m depth. A distinct zone of enhanced
313 turbidity was observed on the continental margin between 200-350 m water depth.



314

315 **Figure 5** CTD transect across the Angolan margin. Shown are data for (a) potential temperature ($^{\circ}\text{C}$), (b) salinity (PSU), (c)
 316 dissolved oxygen concentration (ml l^{-1}), (d) fluorescence (mg m^{-3}), (e) turbidity (NTU) (data plotted using Ocean Data View
 317 v.4.7.8; <http://odv.awi.de>; Schlitzer, 2011). The depth occurrence of CWC mounds is marked by a red, dashed line, the lander
 318 deployments are indicated by colored dots.

319 3.2 Near bottom environmental data

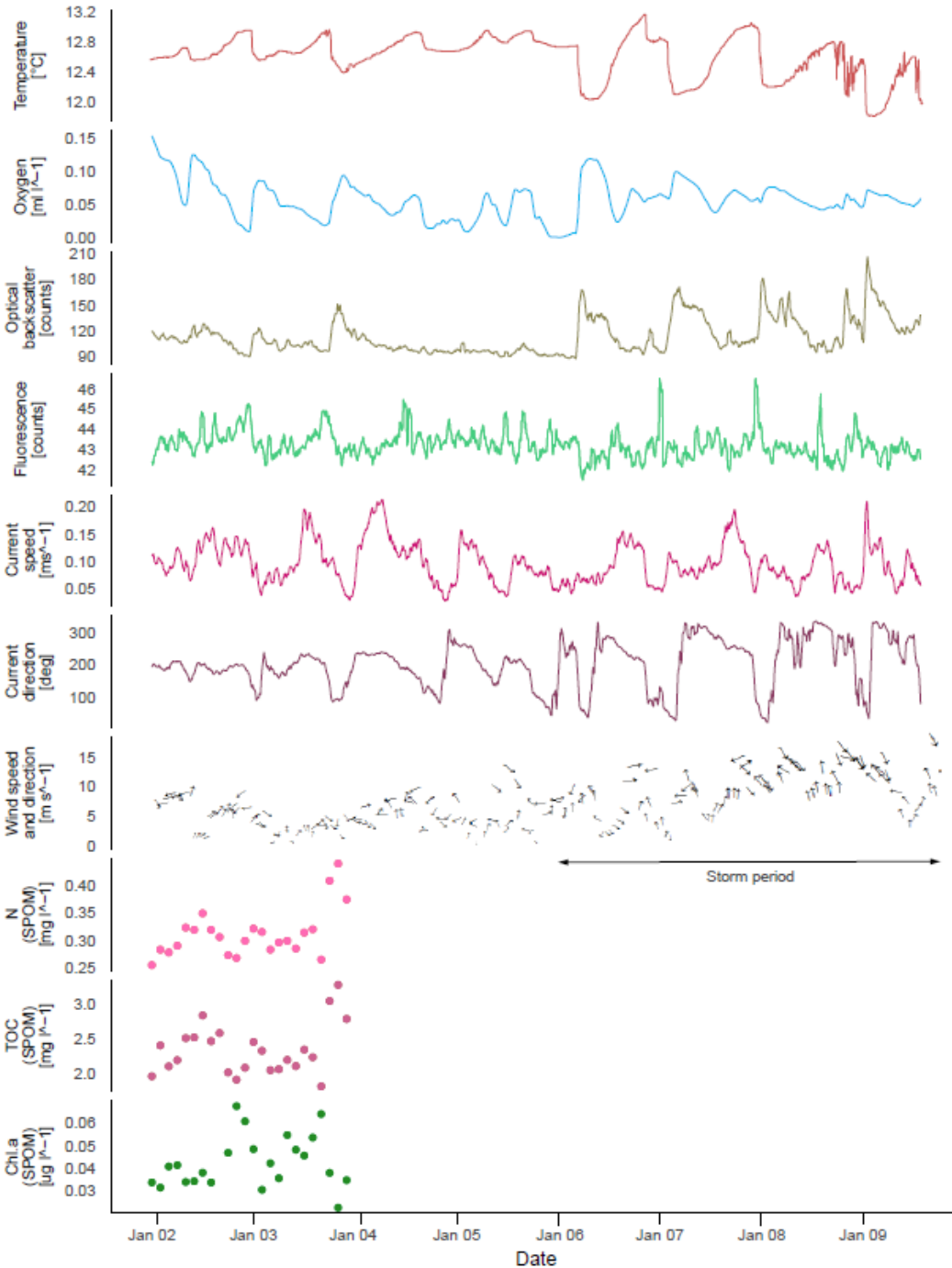
320 3.2.1 Namibian margin

321 Bottom temperature ranged from $11.8\text{--}13.2\text{ }^{\circ}\text{C}$ during the deployment of the ALBEX lander (Table 2, Fig.
 322 6) showing oscillating fluctuations with a maximum semidiurnal ($\Delta T \sim 6\text{ h}$) change of $\sim \Delta 1\text{ }^{\circ}\text{C}$ (on
 323 9.1.2016). The DO concentrations fluctuated between $0\text{--}0.15\text{ ml l}^{-1}$ and was negatively correlated with
 324 temperature ($r=-0.39$, $p<0.01$). Fluorescence ranged from $42\text{--}45\text{ NTU}$ during the deployment and was
 325 positively correlated with temperature ($r=0.38$, $p<0.01$). Hence, both temperature and fluorescence
 326 were negatively correlated with DO concentrations ($r=-0.39$, $p<0.01$) and turbidity (optical backscatter,
 327 $r=-0.35$, $p<0.01$). Turbidity was low until it increased markedly during the second half of the deployment.
 328 During this period on the 6th of January wind speed increased from 10 m s^{-1} to a maximum of 17 m s^{-1}
 329 and remained high for the next six days. The wind direction changed from anticlockwise cyclonic

330 rotation towards alongshore winds. During the strong wind period, colder water (correlation between
331 wind speed and water temperature, $r=-0.55$, $p<0.01$), with a higher turbidity (correlation of wind speed
332 and turbidity, $r=0.42$, $p<0.01$) and on average higher DO concentrations was present. The SLM lander
333 recorded an average pH of 8.01.

334 Maximum current speeds measured during the deployment period were 0.21 m s^{-1} , with average
335 current speeds of 0.09 m s^{-1} (Table 2). The tidal cycle explained $>80\%$ of the pressure fluctuations (Table
336 3), with a semidiurnal signal, M2 (principal lunar semi-diurnal), generating an amplitude of $>0.35 \text{ dbar}$
337 and thus being the most important constituent. Before the 6th of January the current direction oscillated
338 between SW and SE after which it changed to a dominantly northerly current direction (Fig. 6).

339 The observed fluctuations in bottom water temperature at the deployment site imply a vertical tidal
340 movement of around 70 m. This was estimated by comparing the temperature change recorded by the
341 lander to the respective temperature-depth gradient based on water column measurements (CTD site
342 GeoB20553, $12.58 \text{ }^\circ\text{C}$ at 245 m, $12.93 \text{ }^\circ\text{C}$ at 179 m). Due to these vertical tidal movements, the oxygen
343 depleted water from the core of the OMZ is regularly being replaced with somewhat colder and slightly
344 more oxygenated water (Δ up to 0.2 ml l^{-1}).



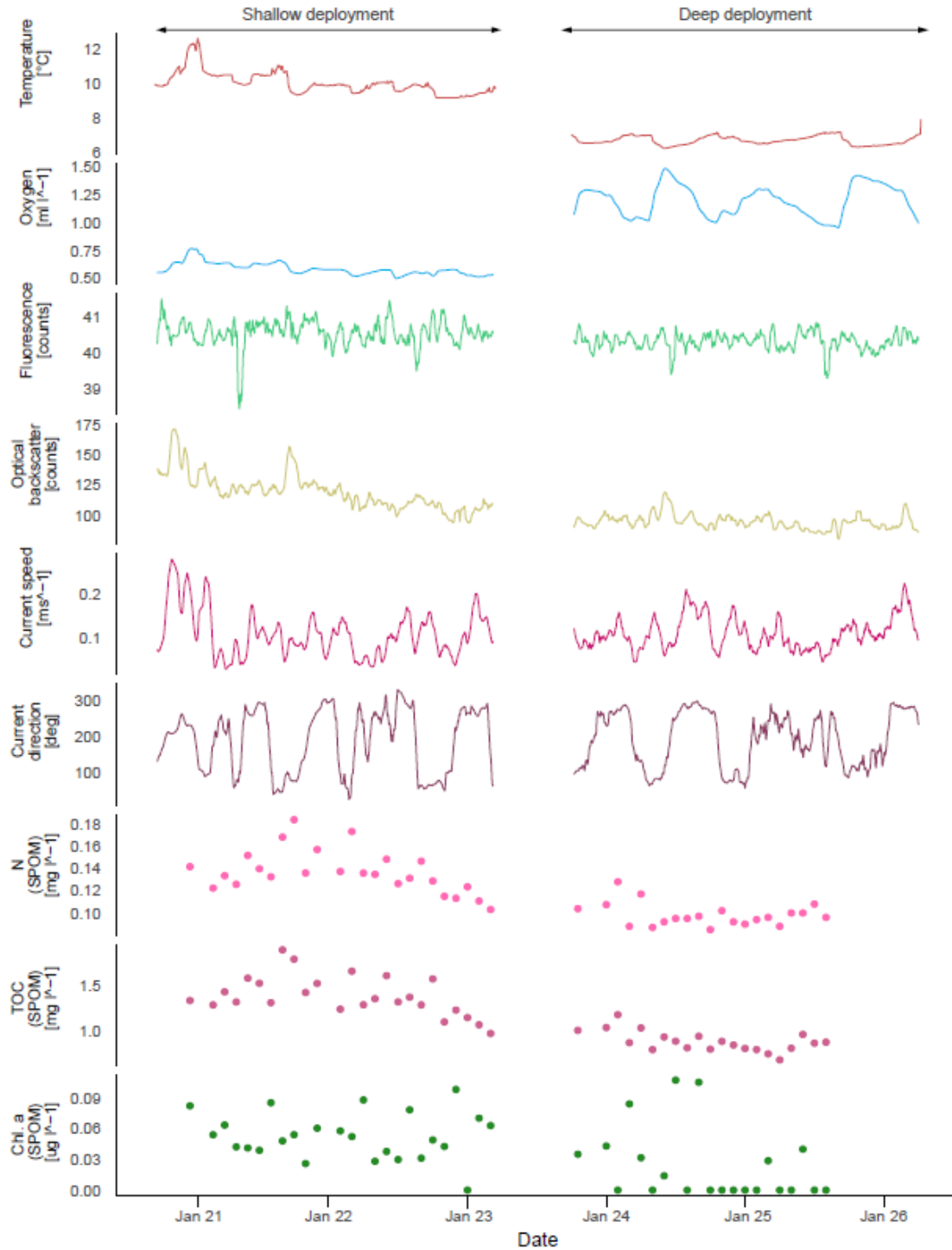
345

346 **Figure 6** Data recorded by the ALBEX lander (210 m) at the Namibian margin in January 2016. Shown are data for temperature
 347 (°C; red), dissolved oxygen concentrations (ml l⁻¹; blue), optical backscatter (turbidity; moss green), fluorescence (counts per
 348 second green), current speed (m s⁻¹; pink), current direction (degree: 0-360°; dark red) as well as nitrogen (mg l⁻¹; pink dots),
 349 carbon (mg l⁻¹; purple dots), and chlorophyll-α concentration (µg l⁻¹; green dots) of SPOM collected during the first 48h by the
 350 McLane pump. These data are supplemented by wind speed and direction (small black arrows) recorded concurrently to the
 351 lander deployment by ship bound devices. Note that current directions changed from a generally south-poleward to an
 352 equatorward direction when wind speed exceeded 10 m s⁻¹ (stormy period indicated by black arrow).

353 *3.2.2 Angolan margin*

354 Mean bottom water temperatures were 6.73 °C at the deeper site (530 m) and 10.06 °C at the shallower
355 site (340 m, Fig. 7, Table 2). The maximum semidiurnal ($\Delta T \sim 6h$) temperature change was $\Delta 1.60$ °C at
356 the deepest site and $\Delta 2.4$ °C at the shallow site (Fig. 7). DO concentrations at the deep site were a factor
357 of two higher than those at the shallow site, i.e. 0.9-1.5 vs. 0.5-0.8 ml l⁻¹ respectively (\cong range between
358 4-14% saturation of both sites), whereas the range of diurnal fluctuations was much smaller compared
359 to the shallow site. DO concentrations were negatively correlated with temperature at the deep site ($r=-$
360 0.99, $p<0.01$) while positively correlated at the shallow site ($r=0.91$, $p<0.01$). Fluorescence was low
361 during both deployments and showed only small fluctuations, being slightly higher at the shallow site
362 (between 38.5 and 41.5 NTU at both sites). Current speeds were relatively high (between 0-0.3 m s⁻¹,
363 average 0.1 m s⁻¹) and positively correlated with temperature at the shallow site ($r=0.31$, $p<0.01$) and
364 negatively correlated at the deep site ($r=-0.22$, $p<0.01$). Analysis of the tidal cycle showed that it
365 explained 29.8-54.9% of the horizontal current fluctuations. The M2 amplitude was 0.06-0.09 m s⁻¹ and
366 was the most important signal (Table 3). A decrease in turbidity was observed during the deployment at
367 the shallow station. This station was located directly below the turbidity maximum between 200-350 m
368 depth as observed in the CTD transect (Fig.5). In contrast, a relative constant and low turbidity was
369 observed for the deep deployment. Turbidity during both deployments was positively correlated to DO
370 concentrations ($r=0.47$, $p<0.01$, shallow deployment and $r=0.50$, $p<0.01$, deep deployment). The SLM
371 lander recorded an average pH of 8.12.

372 The short-term temperature fluctuations imply a vertical tidal movement of around 130 m (12.9-9.1 °C
373 measured by lander \cong 218-349 m depth in CTD above lander at station GeoB20966).



374

375 **Figure 7** Lander data (ALBEX) recorded during at the shallow (~340 m water depth) and deep sites (~530 m water depth) off
 376 Angola (January 2016). Shown are temperature (°C; red), dissolved oxygen concentration (ml l⁻¹; blue), fluorescence (counts per
 377 second; green), optical backscatter (turbidity; yellow), current speed (m s⁻¹; pink) and current direction (degree: 0-360°; purple)
 378 as well as nitrogen (mg l⁻¹; pink dots), carbon (mg l⁻¹; purple dots), and chlorophyll-α concentration (µg l⁻¹; green dots) of SPOM
 379 collected during the both deployments by the McLane pump.

380 3.3 Suspended particulate matter

381 3.3.1 Namibian margin

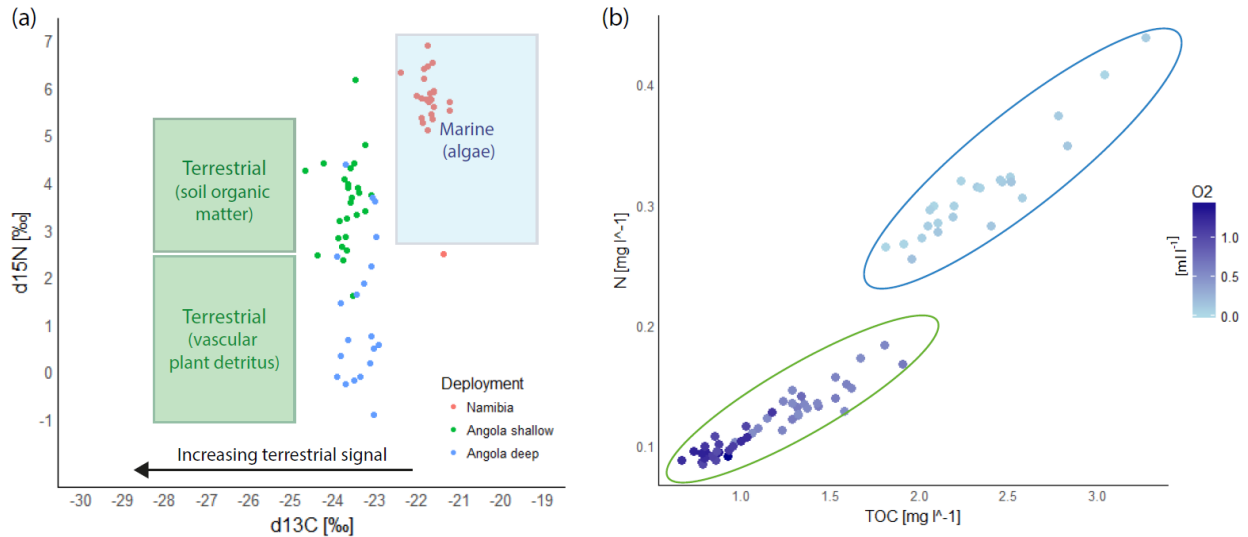
382 The nitrogen (N) concentration of the SPOM measured on the filters of the McLane pump fluctuated
383 between 0.25 and 0.45 mg l⁻¹ (Fig 8). The highest N concentration corresponded with a peak in turbidity
384 ($r=0.42$, $p<0.01$). The $\delta^{15}\text{N}$ values of the lander time series fluctuated between 5.1 and 6.9 with an
385 average value of 5.7 ‰. Total Organic Carbon (TOC) showed a similar pattern as nitrogen, with relative
386 concentrations ranging between 1.8-3.5 mg l⁻¹. The $\delta^{13}\text{C}$ value of the TOC increased during the surveyed
387 time period from -22.39 to -21.24‰ with an average of -21.7 ‰ (Fig. 8a). The C/N ratio ranged from 8.5-
388 6.8 and was on average 7.4 (Fig 8b). During periods of low temperature and more turbid conditions TOC
389 and N as well as the $\delta^{13}\text{C}$ values of the SPOM were higher.

390 Chlorophyll- α concentrations of SPOM were on average 0.042 $\mu\text{g l}^{-1}$ and correlated with the record of
391 the fluorescence ($r=0.43$, $p=0.04$). A six times higher amount of chlorophyll- α degradation products were
392 found during the lander deployment (0.248 $\mu\text{g l}^{-1}$) compared to the amount of chlorophyll- α , giving a
393 $\Sigma\text{Phaeopigment/ Chlorophyll-}\alpha$ ratio of 6.5 (not shown). Additionally, carotenoids (0.08-0.12 $\mu\text{g l}^{-1}$) and
394 fucoxanthin (0.22 $\mu\text{g l}^{-1}$), which are common in diatoms, were major components of the pigment
395 fraction. Zeaxanthin, indicating the presence of prokaryotic cyanobacteria, was only observed in small
396 quantities (0.066 $\mu\text{g l}^{-1}$).

397 3.3.2 Angolan margin

398 In general TOC and N concentrations of SPOM were higher at the shallow compared to the deep site.
399 Nitrogen concentrations varied around 0.14 mg l⁻¹ at 340 m and around 0.1 mg l⁻¹ at 530 m depth (Fig.
400 8b). The $\delta^{15}\text{N}$ values at the shallow site ranged from 1.6-6.2 ‰ (3.7 ‰ average) and were even lower
401 deeper in the water column, viz. range 0.3-3.7 ‰ with an average of 1.4 ‰. The TOC concentrations
402 were on average 1.43 mg l⁻¹ at 340 m and 0.9 mg l⁻¹ at 530 m, with corresponding $\delta^{13}\text{C}$ values ranging
403 between -23.0 and -24.2 (average of -23.6 ‰) at the shallow and between -22.9 and -23.9 (average -
404 23.4 ‰) at the deep site.

405 The chlorophyll- α concentrations of the SPOM collected by the McLane pump varied between 0.1 and
406 0.02 $\mu\text{g l}^{-1}$, with average $\Sigma\text{Phaeopigment/ Chlorophyll-}\alpha$ ratios of 2.6 and 0.5 at the shallow and deep
407 site, respectively. Phytopigments recorded by the shallow deployment included 0.3 $\mu\text{g l}^{-1}$ of fucoxanthin,
408 while at the deep site only a concentration of 0.1 $\mu\text{g l}^{-1}$ was found. No zeaxanthin was recorded in the
409 pigment fraction.



410

411 **Figure 8** Composite records of SPOM collected by the McLane pump of the ALBEX lander at the Namibian and Angolan margins
 412 during all three deployments. (a) $\delta^{15}\text{N}$ and $\delta^{13}\text{C}$ isotopic values at the Namibian (red dots) and Angolan (blue and green dots)
 413 margins. Indicated by the square boxes are common isotopic values of terrestrial and marine organic matter (Boutton 1991,
 414 Holmes et al. 1997, Sigman et al. 2009). The relative contribution of terrestrial material (green boxes) is increasing with a more
 415 negative $\delta^{13}\text{C}$ value. (b) Total organic carbon (TOC) and nitrogen (N) concentration of the SPOM. Values of the Namibian margin
 416 are marked by a blue circle (C/N ratio = 7.8), values of the Angolan margin are marked by a green circle (C/N ratio = 9.6).
 417 Dissolved oxygen concentrations are included to show the higher nutrient concentrations in less oxygenated water.

418 4. Discussion

419 Even though the ecological-niche factor analysis of Davies et al. (2008) and Davies and Guinotte (2011)
 420 predict *L. pertusa* to be absent along the oxygen-limited southwestern African margin, CWC mounds with
 421 two distinct benthic ecosystems were found. The coral mounds on the Namibian shelf host no living CWCs,
 422 instead dead coral framework covering the mounds was overgrown with fauna dominated by bryozoans
 423 and sponges. Along the slope of the Angolan margin an extended coral mound area with thriving CWC
 424 communities was encountered. It is probably that differences in present-day environmental conditions
 425 between the areas influence the faunal assemblages inhabiting them. The potential impact of the key
 426 environmental factors will be discussed below.

427 4.1 Short-term vs long-term variations in environmental properties

428 On the Namibian margin, seasonality has a major impact on local-mid-depth oxygen concentration due
 429 to the periodically varying influence of the Angola current and its associated low DO concentrations
 430 (Chapman and Shannon, 1987). The lowest DO concentration is expected from February to May when
 431 SACW is the dominating water mass on the Namibian margin and the contribution of ESACW is smaller

432 (Mohrholz et al., 2008). Due to this seasonal pattern, the DO concentrations measured in this study
433 (January; Fig. 4) probably do not represent minimum concentrations, which are expected to occur in the
434 following months, but nevertheless give a valuable impression about the extent of the OMZ (February to
435 May; Mohrholz et al., 2014). Interestingly, we captured a flow reversal after the 6th of January from a
436 southward to an equatorward current direction during high wind conditions on the Namibian margin
437 (Fig. 6), leading to an intrusion of ESACW with higher DO concentrations ($\Delta 0.007 \text{ ml l}^{-1}$ on average) and
438 lower temperatures ($\Delta 0.23 \text{ }^\circ\text{C}$ on average, Fig. 5) than the SACW. This led to a temporal increase in the
439 DO concentrations. This shows that variations in the local flow field have the capability to change water
440 properties on relatively short time scales, which might provide an analogue to the water mass variability
441 related to the different seasons (Mohrholz et al., 2008). Such relaxations are possibly important for the
442 survival of the abundant benthic fauna present on the relict coral mounds (Gibson et al., 2003). Other
443 seasonal changes, like riverine outflow do not have decisive impacts on the ecosystem since only
444 relatively small rivers discharge from the Namibian margin. This is also reflected by the dominant marine
445 isotopic signature of the isotopic ratios of $\delta^{15}\text{N}$ and $\delta^{13}\text{C}$ of the SPOM at the mound areas (Fig. 8, cf.
446 Tyrrell and Lucas, 2002).

447 Flow reversals were not observed during the lander deployments on the Angolan margin, where winds
448 are reported to be weak throughout the year providing more stable conditions (Shannon, 2001). Instead
449 river outflow seems to exert a strong influence on the DO concentrations on the Angolan margin. The
450 run-off of the Cuanza and Congo river reach their seasonal maximum in December and January (Kopte et
451 al., 2017), intensifying upper water column stratification. This stratification is restricting vertical mixing
452 and thereby limits ventilation of the oxygen depleted subsurface water masses. In addition rivers
453 transport terrestrial organic matter to the margin, which is reflected by the isotopic signals of the SPOM
454 (-1 to 3‰; Montoya, 2007) which is well below the average isotopic ratio of the marine waters of 5.5 ‰
455 (Meisel et al., 2011). Also $\delta^{13}\text{C}$ values are in line with the $\delta^{13}\text{C}$ values of terrestrial matter which is on
456 average -27 ‰ in this area (Boutton, 1991; Mariotti et al., 1991). The C/N ratio of SPOM is higher
457 compared to material from the Namibian margin, also confirming admixing of terrestrial matter (Perdue
458 and Koprivnjak, 2007). This terrestrial matter contains suitable food sources as well as less suitable food
459 sources, like carbon rich polymeric material (cellulose, hemicellulose and lignin) which cannot easily be
460 taken up by marine organisms (Hedges and Oades, 1997). The combined effects of decreased vertical
461 mixing and additional input of organic matter potentially result in the lowest DO concentrations of the
462 year during the investigated time period (January), since the highest river outflow and therefore
463 strongest stratification is expected during this period.

464 *4.2 Main stressors – Oxygen and temperature*

465 Environmental conditions marked by severe hypoxia and temporal anoxia ($<0.17 \text{ ml l}^{-1}$) likely explain the
466 present-day absence of living CWCs along the Namibian margin. During the measurement period the DO
467 concentrations off Namibia were considerably lower than thus far recorded minimum concentrations
468 near living CWCs ($1\text{-}1.3 \text{ ml l}^{-1}$), which were found off Mauritania where only isolated living CWCs are
469 found (Ramos et al., 2017). Age dating of the Namibian fossil coral framework showed that CWCs
470 disappeared about 5 ka BP, which coincides with an intensification in upwelling and therefore most
471 likely a decline of DO concentrations (Tamborrino et al., accepted), supporting the assumption that the
472 low DO concentrations are responsible for the demise of CWCs on the Namibian margin. Although no
473 living corals were observed on the Namibian coral mounds, we observed a dense living community
474 dominated by sponges and bryozoans (Hebbeln et al., 2017). Several sponge species have been reported
475 to survive at extremely low DO concentrations within OMZs. For instance, along the lower boundary of
476 the Peruvian OMZ sponges were found at DO concentrations as low as $0.06\text{-}0.18 \text{ ml l}^{-1}$ (Mosch et al.,
477 2012). Mills et al. (2018) recently found a sponge (*Tethya wilhelma*) to be physiologically almost
478 insensitive to oxygen stress and to respire aerobically under low DO concentrations (0.02 ml l^{-1}). Sponges
479 can potentially stop their metabolic activity during unfavorable conditions and re-start their metabolism
480 when some oxygen becomes available, for instance during diurnal irrigation of water with somewhat
481 higher DO concentrations. The existence of a living sponge community off Namibia might therefore be
482 explained by the diurnal tides occasionally flushing the sponges with more oxic water enabling them to
483 metabolize, when food availability is highest (Figs. 6). Increased biomass and abundances in these
484 temporary hypoxic-anoxic transition zones were already observed for macro- and mega-fauna in other
485 OMZs and is referred to as the “edge effect” (Mullins et al., 1985; Levin et al., 1991; Sanders, 1969). It is
486 very likely that this mechanism plays a role for the benthic communities on the Namibian as well as the
487 Angolan margin.

488 Along the Angolan margin low oxygen concentrations apparently do not restrict the proliferation of
489 thriving CWC reefs even though DO concentrations are considered hypoxic ($0.5\text{-}1.5 \text{ ml l}^{-1}$). The DO
490 concentrations measured off Angola are well below the lower DO concentration limits for *L. pertusa* based
491 on laboratory experiments and earlier field observations (Schroeder, 2002; Brooke and Ross, 2014). The
492 DO concentrations encountered at the shallow mound sites ($<0.8 \text{ ml l}^{-1}$) are even below the so far lowest
493 limits known for single CWC colonies from the Mauritanian margin (Ramos et al., 2017b). Since in the
494 present study, measured DO concentrations were even lower than the earlier established lower limits this

495 could suggest a much higher tolerance of *L. pertusa* to oxygen levels as low as 0.5 ml l⁻¹ at least in a limited
496 time-period (4% O₂ saturation)

497 In addition to oxygen stress, heat stress is expected to put additional pressure on CWCs. Temperatures at
498 the CWC mounds off Angola ranged from 6.4- 12.6 °C, with the upper limit being close to reported
499 maximum temperatures (~12-14.9 °C; Davies and Guinotte 2011) and are hence expected to impair the
500 ability of CWCs to form mounds (see Wienberg and Titschack 2017). The CWCs were also occurring outside
501 of the expected density envelope of 27.35-27.65 kg m⁻³ in densities well below 27 kg m⁻³ (Fig. 3, Dullo et
502 al., 2008). In most aquatic invertebrates respiration rates roughly double with every 10 °C increase (Q_{10}
503 temperature coefficient = 2-3, e.g. Coma 2002), which at the same time doubles energy demand. Dodds
504 et al. (2007) found a doubling of the respiration rate of *L. pertusa* with an increase at ambient temperature
505 of only 2 °C (viz. Q_{10} = 7-8). This would limit the survival of *L. pertusa* at high temperatures to areas where
506 the increased demand in energy (due to increased respiration) can be compensated by high food
507 availability. Higher respiration rates also imply that enough oxygen needs to be available for the increased
508 respiration. However this creates a negative feedback, since with increased food availability and higher
509 temperatures the oxygen concentration will decrease due to bacterial decomposition of organic
510 substances.

511 Survival of *L. pertusa* under hypoxic conditions along the shallow Angolan CWC areas is probably positively
512 influenced by the fact that periods of highest temperatures coincide with highest DO concentrations
513 during the tidal cycle. Probably here the increase of one stressor is compensated by a reduction of another
514 stressor. On the Namibian margin and the deeper Angolan mound sites the opposite pattern was found,
515 with highest temperatures during lowest DO concentrations. However, at the deeper Angolan mound sites
516 DO concentrations are higher and temperatures more within a suitable range compared to the shallow
517 sites (0.9-1.5 ml l⁻¹, 6.4-8 °C, Fig. 7). Additionally it was shown by ex situ experiments that *L. pertusa* is able
518 to survive periods of hypoxic conditions similar to those found along the Angolan margin for several days,
519 which could be crucial in periods of most adverse conditions (Dodds et al., 2007).

520 **4.3 Food supply**

521 As mentioned above, environmental stresses like high temperature or low DO concentration results in a
522 loss of energy (Odum, 1971; Sokolova et al., 2012), which needs to be balanced by an increased energy
523 (food) availability. Food availability therefore plays a significant role for faunal abundance under hypoxia
524 or unfavorable temperatures (Diaz and Rosenberg, 1995). Above, we argued that survival of sponges and
525 bryozoans on the relict mounds off Namibia and of CWCs, and their associated fauna at the Angolan

526 margin, may be partly due to a high input of high-quality organic matter, compensating the oxygen and
527 thermal stresses. The importance of the food availability for CWCs was already suggested by Eisele et al.
528 (2011), who mechanistically linked CWC mound growth periods with enhanced surface water productivity
529 and hence organic matter supply. Here we found evidence for high quality and quantity of SPOM in both
530 areas indicated by high TOC and N concentrations (Figs. 6 and 7) in combination with a low C/N ratio (Fig.
531 8), a low isotopic signature of $\delta^{15}\text{N}$ and only slightly degraded pigments.

532 The Namibian margin is known for its upwelling cells, where phytoplankton growth is fueled by nutrients
533 from deeper water layers producing high amounts of phytodetritus (Chapman and Shannon, 1985), which
534 subsequently sinks down to the relict mounds on the slope. Benthic communities on the mounds off
535 Namibia occur at relatively shallow depths, hence downward transport of SPOM from the surface waters
536 is rapid and time for decomposition of the sinking particles in the water column is limited. The higher
537 turbidity during lower current speeds provides additional evidence that the material settling from the
538 surface is not transported away with the strong currents (Fig. 6).

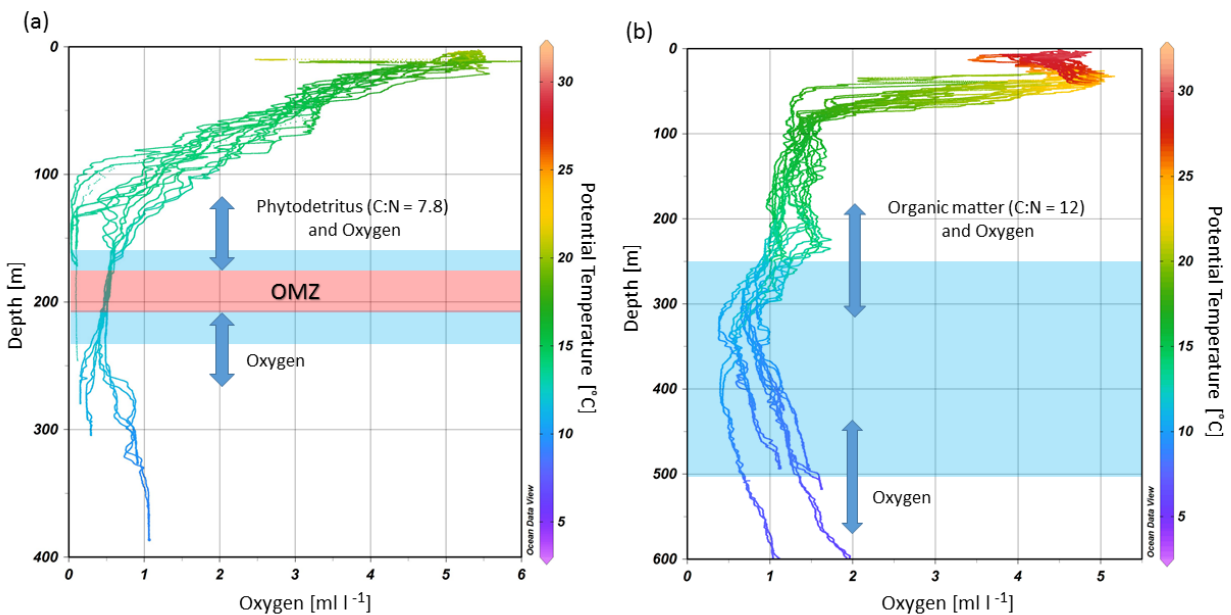
539 At the Angolan coral mounds, SPOM appeared to have a signature corresponding to higher quality organic
540 matter compared to off Namibia. The phytopigments were less degraded and the $\delta^{15}\text{N}$, TOC and N
541 concentration of the SPOM was lower. However, here lower $\delta^{15}\text{N}$ and higher $\Sigma\text{phaeopigment}/\text{chlorophyll-}$
542 α ratio are likely connected to a mixture with terrestrial OM input, which might constitute a less suitable
543 food source for CWCs (Hedges and Oades, 1997). On the other hand the riverine input delivers dissolved
544 nutrients, which can support the growth of phytoplankton, indirectly influencing food supply
545 (Kiriakoulakis et al., 2007; Mienis et al., 2012). Moreover, the variations in food quality at the shallow
546 Angolan reefs, which were relatively small during this study, did not seem to be related to the presence
547 of other environmental stressors. At the Angolan margin we see a rather constant availability of SPOM.
548 The slightly higher turbidity during periods of highest DO concentrations (Fig. 7), suggest that the SPOM
549 on the Angolan margin originates from the bottom nepheloid layer on the margin directly above the CWC
550 mounds (Fig. 5e), which may represent a constant reservoir of fresh SPOM. This reservoir is probably
551 fueled by directly sinking as well as advected organic matter from the surface ocean.

552 *4.4 Tidal currents*

553 The semidiurnal tidal currents observed probably play a major role in the survival of benthic fauna on the
554 SW African margin. On the Namibian margin internal waves deliver oxygen from the surface and deeper
555 waters to the OMZ and thereby enabling benthic fauna on the fossil coral framework to survive in hypoxic
556 conditions (Fig. 9a). At the same time these currents are probably responsible for the delivery of fresh

557 SPOM from the surface productive zone to the communities on the margin, since they promote mixing
558 between the water masses as well as they vertically displace the different water layers.

559 On the Angolan margin internal tides produce slightly faster currents and vertical excursions of up to 130
560 m which are twice as high as those on the Namibian margin. Similar to the Namibian margin these tidal
561 excursions deliver oxygen from shallower and deeper waters to the mound zone and thereby deliver
562 water with more suitable characteristics over the whole extend of the parts of the OMZ which otherwise
563 may be unsuitable for CWCs (Fig. 9b). Internal tides are also responsible for the formation of a bottom
564 nepheloid layer in 200-350 m depth (Fig. 5e). This layer is formed by trapping of organic matter as well as
565 bottom erosion due to turbulences created by the interaction of internal waves with the margin
566 topography, which intensifies near-bottom water movements. These internal waves are able to move on
567 the density gradient between water masses, which are located in 225 and 300 m depth (Fig. 3). Tidal
568 waves will be amplified due to a critical match between the characteristic slope of the internal M2 tide
569 and the bottom slope of the Angolan margin, as is known from other continental slope regions (Dickson
570 and McCave, 1986; Mienis et al., 2007). As argued above, this turbid layer is likely important for the
571 nutrition of the slightly deeper situated CWC mounds, since vertical mixing is otherwise hindered by the
572 strong stratification.



573

574 **Figure 9** Depth range of cold-water coral mound occurrences (blue shaded areas) at the (a) Namibian and (b) Angolan margins
575 in relation to the dissolved oxygen concentrations and potential temperature. Diurnal tides are delivering mainly phytodetritus

576 (shown in (a) and organic matter from the benthic nepheloid layer (shown in (b) as well as oxygen from above, and from below
577 to the mound sites (indicated by blue arrows, the length of which indicate the tidal ranges).

578 5. Conclusions

579 Different environmental properties explain the present conditions of the benthic communities on the
580 southwestern African margin including temperature, DO concentration, food supply and tidal
581 movements. The DO concentrations probably define the limits of a suitable habitat for CWCs along the
582 Namibian and the Angolan margin, whereas high temperatures constitute additional stress by increasing
583 the respiration rate and therefore energy demand. On the Namibian margin, where DO concentrations
584 dropped below 0.01 ml l^{-1} , only fossil CWC mounds covered by a community dominated by sponges and
585 bryozoans were found. This benthic community survives as it receives periodically waters with slightly
586 higher DO concentrations ($>0.03 \text{ ml l}^{-1}$) due to regular tidal oscillations (semi diurnal) and erratic wind
587 events (seasonal). At the same time, a high quality and quantity of SPOM sinking down from the surface
588 water mass enables the epifaunal community to survive despite the oxygen stress and sustain its
589 metabolic energy demand at the Namibian OMZ, while CWCs are not capable to withstand such extreme
590 conditions. In contrast, thriving CWCs on the Angolan coral mounds were encountered despite the
591 overall hypoxic conditions. The DO concentrations were slightly higher than those on the Namibian
592 margin, but nevertheless below the lowest threshold that was so far reported for *L. pertusa* (Ramos et
593 al., 2017; Davies et al., 2010; Davies et al., 2008). In combination with temperatures, close to the upper
594 limits for *L. pertusa*, metabolic energy demand probably reached a maximum. High energy requirements
595 might have been compensated by the general high availability of fresh resuspended SPOM. Fresh SPOM
596 accumulates on the Angolan margin just above the CWC area and is regularly supplied due to mixing by
597 semidiurnal tidal currents, despite the restricted sinking of SPOM from the surface due to the strong
598 stratification.

599 CWC and sponge communities are known to play an important role as a refuge, feeding ground and
600 nursery for commercial fishes (Miller et al., 2012) and have a crucial role in the marine benthic pelagic
601 coupling (Cathalot et al., 2015). Their ecosystem services are threatened by the expected expansion of
602 OMZs due to anthropogenic activities like rising nutrient loads and climate change (Breitburg et al.,
603 2018). This study showed that benthic fauna is able to cope with low oxygen levels as long as sufficient
604 high quality food is available. Further, reef associated sponge grounds, as encountered on the Namibian
605 margin could play a crucial role in taking over the function of CWCs in marine carbon cycling as well as in
606 providing a habitat for associated fauna, when conditions become unsuitable for CWCs.

607 6. Data availability

608 Data will be uploaded to Pangea after publication.

609

610 7. Author contribution

611 UH analyzed the physical and chemical data, wrote the manuscript and prepared the figures with
612 contributions of all authors. FM, GD and ML designed the lander research. DH and CW led the cruise and
613 wrote the initial cruise plan. FM and ML collected the data during the research cruise. WCD was
614 responsible for water column measurements with the CTD. AF and ML provided habitat characteristics,
615 including species identification of both CWC areas. KJ performed the tidal analysis and provided
616 together with SF data of the SML lander. All authors contributed to the data interpretation and
617 discussion of the manuscript.

618

619 8. Competing interests

620 The authors declare that they have no conflict of interest.

621

622 9. Acknowledgements

623 We thank the Captain of the RV *Meteor* cruise M122, Rainer Hammacher, his officers and crew, which
624 contributed to the success of this cruise. We also like to thank the scientific and technical staff for their
625 assistance during the cruise and the work in the laboratory. Greatly acknowledged are the efforts from
626 the German Diplomatic Corps in the German Embassies in Windhoek and Luanda and in the Foreign
627 Office in Berlin. We thank the German Science Foundation (DFG) for providing ship time on RV *Meteor*
628 and for funding the ROV *Squid* operations to investigate the cold-water coral ecosystems off Angola and
629 Namibia. This work was further supported through the DFG Research Center/ Cluster of Excellence
630 “MARUM – The Ocean in the Earth System”. UH is funded by the SponGES project, which received
631 funding from the European Union's Horizon 2020 research and innovation program under grant
632 agreement No 679849. FM is supported by the Innovational Research Incentives Scheme of the
633 Netherlands Organisation for Scientific Research (NWO-VIDI grant 016.161.360). GJR is supported by the
634 Netherlands Earth System Science Centre (NESSC), financially supported by the Ministry of Education,
635 Culture and Science (OCW). KJ is funded through the FATE project (Fate of cold-water coral reefs –
636 identifying drivers of ecosystem change), supported by the Norwegian Research Council (NRC).

637 10. References

- 638 Boutton, T. W.: Stable carbon isotope ratios of natural materials: II. Atmospheric, terrestrial, marine, and
639 freshwater environments, *Carbon isotope techniques*, 1, 173, 1991.
- 640 Breitburg, D., Levin, L. A., Oschlies, A., Grégoire, M., Chavez, F. P., Conley, D. J., Garçon, V., Gilbert, D.,
641 Gutiérrez, D., and Isensee, K.: Declining oxygen in the global ocean and coastal waters, *Science*, 359,
642 eaam7240, 2018.
- 643 Brooke, S., and Ross, S. W.: First observations of the cold-water coral *Lophelia pertusa* in mid-Atlantic
644 canyons of the USA, *Deep Sea Research Part II: Topical Studies in Oceanography*, 104, 245-251, 2014.
- 645 Buhl-Mortensen, L., Vanreusel, A., Gooday, A. J., Levin, L. A., Priede, I. G., Buhl-Mortensen, P.,
646 Gheerardyn, H., King, N. J., and Raes, M.: Biological structures as a source of habitat heterogeneity and
647 biodiversity on the deep ocean margins, *Marine Ecology*, 31, 21-50, 2010.
- 648 Cairns, S. D.: Deep-water corals: an overview with special reference to diversity and distribution of deep-
649 water scleractinian corals, *Bulletin of Marine Science*, 81, 311-322, 2007.
- 650 Carr, M.-E., and Kearns, E. J.: Production regimes in four Eastern Boundary Current systems, *Deep Sea*
651 *Research Part II: Topical Studies in Oceanography*, 50, 3199-3221, 2003.
- 652 Cathalot, C., Van Oevelen, D., Cox, T. J., Kutti, T., Lavaleye, M., Duineveld, G., and Meysman, F. J.: Cold-
653 water coral reefs and adjacent sponge grounds: Hotspots of benthic respiration and organic carbon
654 cycling in the deep sea, *Frontiers in Marine Science*, 2, 37, 2015.
- 655 Cavan, E. L., Trimmer, M., Shelley, F., and Sanders, R.: Remineralization of particulate organic carbon in
656 an ocean oxygen minimum zone, *Nature communications*, 8, 14847, 2017.
- 657 Chapman, P., and Shannon, L.: The Benguela ecosystem, Part II. Chemistry and related processes.
658 *Oceanography and Marine Biology. An Annual Review*, 23, 183-251, 1985.
- 659 Chapman, P., and Shannon, L.: Seasonality in the oxygen minimum layers at the extremities of the
660 Benguela system, *South African Journal of Marine Science*, 5, 85-94, 1987.
- 661 Coma, R.: Seasonality of in situ respiration rate in three temperate benthic suspension feeders,
662 *Limnology and Oceanography*, 47, 324-331, 2002.
- 663 Costello, M. J., McCrea, M., Freiwald, A., Lundälv, T., Jonsson, L., Bett, B. J., van Weering, T. C., de Haas,
664 H., Roberts, J. M., and Allen, D.: Role of cold-water *Lophelia pertusa* coral reefs as fish habitat in the NE
665 Atlantic, in: *Cold-water corals and ecosystems*, Springer, Heidelberg, 771-805, 2005.
- 666 Davies, A. J., Wisshak, M., Orr, J. C., and Roberts, J. M.: Predicting suitable habitat for the cold-water
667 coral *Lophelia pertusa* (Scleractinia), *Deep Sea Research Part I: Oceanographic Research Papers*, 55,
668 1048-1062, 2008.
- 669 Davies, A. J., Duineveld, G. C., Lavaleye, M. S., Bergman, M. J., van Haren, H., and Roberts, J. M.:
670 Downwelling and deep-water bottom currents as food supply mechanisms to the cold-water coral
671 *Lophelia pertusa* (Scleractinia) at the Mingulay Reef Complex, *Limnology and Oceanography*, 54, 620-
672 629, 2009.
- 673 Davies, A. J., Duineveld, G. C., van Weering, T. C., Mienis, F., Quattrini, A. M., Seim, H. E., Bane, J. M., and
674 Ross, S. W.: Short-term environmental variability in cold-water coral habitat at Viosca Knoll, Gulf of
675 Mexico, *Deep Sea Research Part I: Oceanographic Research Papers*, 57, 199-212, 2010.
- 676 Davies, A. J., and Guinotte, J. M.: Global habitat suitability for framework-forming cold-water corals, *PLoS*
677 *one*, 6, e18483, 2011.
- 678 De Haas, H., Mienis, F., Frank, N., Richter, T. O., Steinacher, R., De Stigter, H., Van der Land, C., and Van
679 Weering, T. C.: Morphology and sedimentology of (clustered) cold-water coral mounds at the south
680 Rockall Trough margins, NE Atlantic Ocean, *Facies*, 55, 1-26, 2009.
- 681 Diaz, R. J., and Rosenberg, R.: Marine benthic hypoxia: a review of its ecological effects and the
682 behavioural responses of benthic macrofauna, *Oceanography and Marine Biology. An Annual Review*,
683 33, 245-203, 1995.

684 Dickson, R., and McCave, I.: Nepheloid layers on the continental slope west of Porcupine Bank, Deep Sea
685 Research Part A. Oceanographic Research Papers, 33, 791-818, 1986.

686 Dodds, L., Roberts, J., Taylor, A., and Marubini, F.: Metabolic tolerance of the cold-water coral *Lophelia*
687 *pertusa* (Scleractinia) to temperature and dissolved oxygen change, Journal of Experimental Marine
688 Biology and Ecology, 349, 205-214, 2007.

689 Dodds, L., Black, K., Orr, H., and Roberts, J.: Lipid biomarkers reveal geographical differences in food
690 supply to the cold-water coral *Lophelia pertusa* (Scleractinia), Marine Ecology Progress Series, 397, 113-
691 124, 2009.

692 Duineveld, G. C., Lavaleye, M. S., Bergman, M. J., De Stigter, H., and Mienis, F.: Trophic structure of a
693 cold-water coral mound community (Rockall Bank, NE Atlantic) in relation to the near-bottom particle
694 supply and current regime, Bulletin of Marine Science, 81, 449-467, 2007.

695 Dullo, W.-C., Flögel, S., and Rüggeberg, A.: Cold-water coral growth in relation to the hydrography of the
696 Celtic and Nordic European continental margin, Marine Ecology Progress Series, 371, 165-176, 2008.

697 Eisele, M., Frank, N., Wienberg, C., Hebbeln, D., Correa, M. L., Douville, E., and Freiwald, A.: Productivity
698 controlled cold-water coral growth periods during the last glacial off Mauritania, Marine Geology, 280,
699 143-149, 2011.

700 Fink, H. G., Wienberg, C., Hebbeln, D., McGregor, H. V., Schmiedl, G., Taviani, M., and Freiwald, A.:
701 Oxygen control on Holocene cold-water coral development in the eastern Mediterranean Sea, Deep Sea
702 Research Part I: Oceanographic Research Papers, 62, 89-96, 2012.

703 Flögel, S., Dullo, W.-C., Pfannkuche, O., Kiriakoulakis, K., and Rüggeberg, A.: Geochemical and physical
704 constraints for the occurrence of living cold-water corals, Deep Sea Research Part II: Topical Studies in
705 Oceanography, 99, 19-26, 2014.

706 Frederiksen, R., Jensen, A., and Westerberg, H.: The distribution of the scleractinian coral *Lophelia*
707 *pertusa* around the Faroe Islands and the relation to internal tidal mixing, Sarsia, 77, 157-171, 1992.

708 Freiwald, A.: Reef-forming cold-water corals, in: Ocean margin systems, Springer, 365-385, 2002.

709 Freiwald, A., Fossa, J. H., Grehan, A., Koslow, T., and Roberts, J. M.: Cold water coral reefs: out of sight-
710 no longer out of mind, 2004.

711 Freiwald, A., Beuck, L., Rüggeberg, A., Taviani, M., Hebbeln, D., and Participants, R. V. M. C. M.-. The
712 white coral community in the central Mediterranean Sea revealed by ROV surveys, Oceanography, 22,
713 58-74, 2009.

714 Geissler, W., Schwenk, T., and Wintersteller, P.: Walvis Ridge Passive-Source Seismic Experiment
715 (WALPASS) – Cruise No. MSM20/1 – January 06 – January 15, 2012 - Cape Town (South Africa) – Walvis
716 Bay (Namibia), DFG-Senatskommission für Ozeanographie, MARIA S. MERIAN-Berichte, MSM20/1, 54
717 pp., 2013.

718 Gori, A., Grover, R., Orejas, C., Sikorski, S., and Ferrier-Pagès, C.: Uptake of dissolved free amino acids by
719 four cold-water coral species from the Mediterranean Sea, Deep Sea Research Part II: Topical Studies in
720 Oceanography, 99, 42-50, 2014.

721 Grasmueck, M., Eberli, G. P., Viggiano, D. A., Correa, T., Rathwell, G., and Luo, J.: Autonomous
722 underwater vehicle (AUV) mapping reveals coral mound distribution, morphology, and oceanography in
723 deep water of the Straits of Florida, Geophysical Research Letters, 33, 2006.

724 Hebbeln, D., Wienberg, C., Wintersteller, P., Freiwald, A., Becker, M., Beuck, L., Dullo, W.-C., Eberli, G.,
725 Glogowski, S., and Matos, L.: Environmental forcing of the Campeche cold-water coral province,
726 southern Gulf of Mexico, Biogeosciences (BG), 11, 1799-1815, 2014.

727 Hebbeln, D., Wienberg, C., Bender, M., Bergmann, F., Dehning, K., Dullo, W.-C., Eichstädter, R., Flöter, S.,
728 Freiwald, A., Gori, A., Haberkern, J., Hoffmann, L., João, F., Lavaleye, M., Leymann, T., Matsuyama, K.,
729 Meyer-Schack, B., Mienis, F., Moçambique, I., Nowald, N., Orejas, C., Ramos Cordova, C., Saturev, D.,
730 Seiter, C., Titschack, J., Vittori, V., Wefing, A.-M., Wilsenack, M., and Wintersteller, P.: ANNA Cold-Water
731 Coral Ecosystems off Angola and Namibia - Cruise No. M122 - December 30, 2015 - January 31, 2016 -

732 Walvis Bay (Namibia) - Walvis Bay (Namibia), METEOR-Berichte, M122 https://doi.org/10.2312/cr_m122
733 2017.

734 Hedges, J., and Oades, J.: Comparative organic geochemistries of soils and marine sediments, *Organic*
735 *geochemistry*, 27, 319-361, 1997.

736 Henry, L.-A., and Roberts, J. M.: Biodiversity and ecological composition of macrobenthos on cold-water
737 coral mounds and adjacent off-mound habitat in the bathyal Porcupine Seabight, NE Atlantic, *Deep Sea*
738 *Research Part I: Oceanographic Research Papers*, 54, 654-672, 2007.

739 Henry, L.-A., and Roberts, J. M.: Global Biodiversity in Cold-Water Coral Reef Ecosystems, in: *Marine*
740 *Animal Forests*, Springer, 235-256, 2017.

741 Hutchings, L., Van der Lingen, C., Shannon, L., Crawford, R., Verheye, H., Bartholomae, C., Van der Plas,
742 A., Louw, D., Kreiner, A., and Ostrowski, M.: The Benguela Current: An ecosystem of four components,
743 *Progress in Oceanography*, 83, 15-32, 2009.

744 Junker, T., Mohrholz, V., Siegfried, L., and van der Plas, A.: Seasonal to interannual variability of water
745 mass characteristics and currents on the Namibian shelf, *Journal of Marine Systems*, 165, 36-46, 2017.

746 Karstensen, J., Stramma, L., and Visbeck, M.: Oxygen minimum zones in the eastern tropical Atlantic and
747 Pacific oceans, *Progress in Oceanography*, 77, 331-350, 2008.

748 Kiriakoulakis, K., Fisher, E., Wolff, G. A., Freiwald, A., Grehan, A., and Roberts, J. M.: Lipids and nitrogen
749 isotopes of two deep-water corals from the North-East Atlantic: initial results and implications for their
750 nutrition, in: *Cold-water corals and ecosystems*, edited by: Freiwald, A. a. R., J.M. (eds.), Springer,
751 Heidelberg, 715-729, 2005.

752 Kiriakoulakis, K., Freiwald, A., Fisher, E., and Wolff, G.: Organic matter quality and supply to deep-water
753 coral/mound systems of the NW European Continental Margin, *International Journal of Earth Sciences*,
754 96, 159-170, 2007.

755 Kopte, R., Brandt, P., Dengler, M., Tchikalanga, P., Macuéria, M., and Ostrowski, M.: The Angola Current:
756 Flow and hydrographic characteristics as observed at 11° S, *Journal of Geophysical Research: Oceans*,
757 122, 1177-1189, 2017.

758 Kostianoy, A., and Lutjeharms, J.: Atmospheric effects in the Angola-Benguela frontal zone, *Journal of*
759 *Geophysical Research: Oceans*, 104, 20963-20970, 1999.

760 Kraay, G. W., Zapata, M., and Veldhuis, M. J.: Separation of Chlorophylls c1c2, and c3 of marine
761 Phytoplankton by Reverse Phase C18 high Performance liquid Chromatography 1, *Journal of Phycology*,
762 28, 708-712, 1992.

763 Le Guilloux, E., Olu, K., Bourillet, J.-F., Savoye, B., Iglésias, S., and Sibuet, M.: First observations of deep-
764 sea coral reefs along the Angola margin, *Deep Sea Research Part II: Topical Studies in Oceanography*, 56,
765 2394-2403, 2009.

766 Levin, L. A., Huggett, C. L., and Wishner, K. F.: Control of deep-sea benthic community structure by
767 oxygen and organic-matter gradients in the eastern Pacific Ocean, *Journal of Marine Research*, 49, 763-
768 800, 1991.

769 Lutjeharms, J., and Stockton, P.: Kinematics of the upwelling front off southern Africa, *South African*
770 *Journal of Marine Science*, 5, 35-49, 1987.

771 Mariotti, A., Gadel, F., and Giresse, P.: Carbon isotope composition and geochemistry of particulate
772 organic matter in the Congo River (Central Africa): application to the study of Quaternary sediments off
773 the mouth of the river, *Chemical Geology: Isotope Geoscience Section*, 86, 345-357, 1991.

774 Meisel, S., Struck, U., and Emeis, K. C.: Nutrient dynamics and oceanographic features in the central
775 Namibian upwelling region as reflected in $\delta^{15}\text{N}$ -signals of suspended matter and surface sediments,
776 *Fossil Record*, 14, 153-169, 2011.

777 Mienis, F., De Stigter, H., White, M., Duineveld, G., De Haas, H., and Van Weering, T.: Hydrodynamic
778 controls on cold-water coral growth and carbonate-mound development at the SW and SE Rockall

779 Trough Margin, NE Atlantic Ocean, Deep Sea Research Part I: Oceanographic Research Papers, 54, 1655-
780 1674, 2007.

781 Mienis, F., De Stigter, H., De Haas, H., and Van Weering, T.: Near-bed particle deposition and
782 resuspension in a cold-water coral mound area at the Southwest Rockall Trough margin, NE Atlantic,
783 Deep Sea Research Part I: Oceanographic Research Papers, 56, 1026-1038, 2009.

784 Mienis, F., Duineveld, G., Davies, A., Ross, S., Seim, H., Bane, J., and Van Weering, T.: The influence of
785 near-bed hydrodynamic conditions on cold-water corals in the Viosca Knoll area, Gulf of Mexico, Deep
786 Sea Research Part I: Oceanographic Research Papers, 60, 32-45, 2012.

787 Mienis, F., Duineveld, G., Davies, A., Lavaleye, M., Ross, S., Seim, H., Bane, J., Van Haren, H., Bergman,
788 M., and De Haas, H.: Cold-water coral growth under extreme environmental conditions, the Cape
789 Lookout area, NW Atlantic, Biogeosciences, 11, 2543, 2014.

790 Miller, R. J., Hocevar, J., Stone, R. P., and Fedorov, D. V.: Structure-forming corals and sponges and their
791 use as fish habitat in Bering Sea submarine canyons, PLoS One, 7, e33885, 2012.

792 Mills, D. B., Francis, W. R., Vargas, S., Larsen, M., Elemans, C. P., Canfield, D. E., and Wörheide, G.: The
793 last common ancestor of animals lacked the HIF pathway and respired in low-oxygen environments,
794 eLife, 7, e31176, 2018.

795 Mohrholz, V., Bartholomae, C., Van der Plas, A., and Lass, H.: The seasonal variability of the northern
796 Benguela undercurrent and its relation to the oxygen budget on the shelf, Continental Shelf Research,
797 28, 424-441, 2008.

798 Mohrholz, V., Eggert, A., Junker, T., Nausch, G., Ohde, T., and Schmidt, M.: Cross shelf hydrographic and
799 hydrochemical conditions and their short term variability at the northern Benguela during a normal
800 upwelling season, Journal of Marine Systems, 140, 92-110, 2014.

801 Montoya, J. P.: Natural abundance of ^{15}N in marine planktonic ecosystems, Stable isotopes in Ecology
802 and Environmental Science, 176, 2007.

803 Mortensen, P. B., Hovland, T., Fosså, J. H., and Furevik, D. M.: Distribution, abundance and size of
804 *Lophelia pertusa* coral reefs in mid-Norway in relation to seabed characteristics, Journal of the Marine
805 Biological Association of the United Kingdom, 81, 581-597, 2001.

806 Mosch, T., Sommer, S., Dengler, M., Noffke, A., Bohlen, L., Pfannkuche, O., Liebetrau, V., and Wallmann,
807 K.: Factors influencing the distribution of epibenthic megafauna across the Peruvian oxygen minimum
808 zone, Deep Sea Research Part I: Oceanographic Research Papers, 68, 123-135, 2012.

809 Mueller, C., Larsson, A., Veuger, B., Middelburg, J., and Van Oevelen, D.: Opportunistic feeding on
810 various organic food sources by the cold-water coral *Lophelia pertusa*, Biogeosciences, 11, 123-133,
811 2014.

812 Mullins, H. T., Thompson, J. B., McDougall, K., and Vercoutere, T. L.: Oxygen-minimum zone edge effects:
813 evidence from the central California coastal upwelling system, Geology, 13, 491-494, 1985.

814 Odum, H. T.: Environment, power and society, New York, USA, Wiley-Interscience, 1971.

815 Oevelen, D. v., Duineveld, G., Lavaleye, M., Mienis, F., Soetaert, K., and Heip, C. H.: The cold-water coral
816 community as hotspot of carbon cycling on continental margins: A food-web analysis from Rockall Bank
817 (northeast Atlantic), Limnology and Oceanography, 54, 1829-1844, 2009.

818 Perdue, E. M., and Koprivnjak, J.-F.: Using the C/N ratio to estimate terrigenous inputs of organic matter
819 to aquatic environments, Estuarine, Coastal and Shelf Science, 73, 65-72, 2007.

820 Pichevin, L., Bertrand, P., Boussafir, M., and Disnar, J.-R.: Organic matter accumulation and preservation
821 controls in a deep sea modern environment: an example from Namibian slope sediments, Organic
822 Geochemistry, 35, 543-559, 2004.

823 Poole, R., and Tomczak, M.: Optimum multiparameter analysis of the water mass structure in the
824 Atlantic Ocean thermocline, Deep Sea Research Part I: Oceanographic Research Papers, 46, 1895-1921,
825 1999.

826 Rae, C. D.: A demonstration of the hydrographic partition of the Benguela upwelling ecosystem at 26°
827 40'S, African Journal of Marine Science, 27, 617-628, 2005.

828 Ramos, A., Sanz, J. L., Ramil, F., Agudo, L. M., and Presas-Navarro, C.: The Giant Cold-Water Coral
829 Mounds Barrier Off Mauritania, in: Deep-Sea Ecosystems Off Mauritania, edited by: Ramos, A., Ramil, F,
830 Sanz, JL (Eds.), Springer, 481-525, 2017.

831 Roberts, J. M., Wheeler, A. J., and Freiwald, A.: Reefs of the deep: the biology and geology of cold-water
832 coral ecosystems, Science, 312, 543-547, 2006.

833 Ruhl, H. A.: Community change in the variable resource habitat of the abyssal northeast Pacific, Ecology,
834 89, 991-1000, 2008.

835 Sanders, H.: Benthic marine diversity and the stability-time hypothesis, Brookhaven Symposia in Biology,
836 1969, 71-81,

837 Schlitzer, R.: Ocean Data View. <http://odv.awi.de>, 2011.

838 Schroeder, W.: Observations of *Lophelia pertusa* and the surficial geology at a deep-water site in the
839 northeastern Gulf of Mexico, Hydrobiologia, 471, 29-33, 2002.

840 Shannon, L., Boyd, A., Brundrit, G., and Taunton-Clark, J.: On the existence of an El Niño-type
841 phenomenon in the Benguela system, Journal of Marine Research, 44, 495-520, 1986.

842 Shannon, L., Agenbag, J., and Buys, M.: Large-and mesoscale features of the Angola-Benguela front,
843 South African Journal of Marine Science, 5, 11-34, 1987.

844 Shannon, L., and Nelson, G.: The Benguela: large scale features and processes and system variability, in:
845 The South Atlantic, Springer, Berlin, Heidelberg, 163-210, 1996.

846 Shannon, L.: Benguela Current, Ocean Currents: A Derivative of Encyclopedia of Ocean Sciences, 23-34,
847 2001.

848 Sokolova, I. M., Frederich, M., Bagwe, R., Lannig, G., and Sukhotin, A. A.: Energy homeostasis as an
849 integrative tool for assessing limits of environmental stress tolerance in aquatic invertebrates, Marine
850 Environmental Research, 79, 1-15, 2012.

851 Tahey, T., Duineveld, G., Berghuis, E., and Helder, W.: Relation between sediment-water fluxes of
852 oxygen and silicate and faunal abundance at continental shelf, slope and deep-water stations in the
853 northwest Mediterranean, Marine Ecology Progress Series, 119-130, 1994.

854 Tamborrino, L., Wienberg, C., Titschack, J., Wintersteller, P., Mienis, F., Freiwald, A., Orejas, C., Dullo,
855 W.-C., Haberkern, J., and Hebbeln, D.: Mid-Holocene extinction of cold-water corals on the Namibian
856 shelf steered by the Benguela oxygen minimum zone, accepted.

857 Taviani, M., Remia, A., Corselli, C., Freiwald, A., Malinverno, E., Mastrototaro, F., Savini, A., and Tursi, A.:
858 First geo-marine survey of living cold-water *Lophelia* reefs in the Ionian Sea (Mediterranean basin),
859 Facies, 50, 409-417, 2005.

860 R Core Team, R. C.: R: A language and environment for statistical computing [Internet]. Vienna, Austria;
861 2014. 2017.

862 Thiem, Ø., Ravagnan, E., Fosså, J. H., and Berntsen, J.: Food supply mechanisms for cold-water corals
863 along a continental shelf edge, Journal of Marine Systems, 60, 207-219, 2006.

864 Titschack, J., Baum, D., De Pol-Holz, R., Lopez Correa, M., Forster, N., Flögel, S., Hebbeln, D., and
865 Freiwald, A.: Aggradation and carbonate accumulation of Holocene Norwegian cold-water coral reefs,
866 Sedimentology, 62, 1873-1898, 2015.

867 Tyrrell, T., and Lucas, M. I.: Geochemical evidence of denitrification in the Benguela upwelling system,
868 Continental Shelf Research, 22, 2497-2511, 2002.

869 van Haren, H., Mienis, F., Duineveld, G. C., and Lavaleye, M. S.: High-resolution temperature
870 observations of a trapped nonlinear diurnal tide influencing cold-water corals on the Logachev mounds,
871 Progress in Oceanography, 125, 16-25, 2014.

872 van Soest, R. W., Cleary, D. F., de Kluijver, M. J., Lavaleye, M. S., Maier, C., and van Duyl, F. C.: Sponge
873 diversity and community composition in Irish bathyal coral reefs, Contributions to Zoology, 76, 2007.

874 Welschmeyer, N. A., and Lorenzen, C. J.: Chlorophyll budgets: Zooplankton grazing and phytoplankton
875 growth in a temperate fjord and the Central Pacific Gyres¹, *Limnology and Oceanography*, 30, 1-21,
876 1985.

877 Wheeler, A. J., Beyer, A., Freiwald, A., De Haas, H., Huvenne, V., Kozachenko, M., Olu-Le Roy, K., and
878 Opderbecke, J.: Morphology and environment of cold-water coral carbonate mounds on the NW
879 European margin, *International Journal of Earth Sciences*, 96, 37-56, 2007.

880 White, M., Mohn, C., de Stigter, H., and Mottram, G.: Deep-water coral development as a function of
881 hydrodynamics and surface productivity around the submarine banks of the Rockall Trough, NE Atlantic,
882 in: *Cold-water corals and ecosystems*, edited by: A Freiwald, J. R., Springer, Heidelberg, 503-514, 2005.

883 White, M., Wolff, G. A., Lundälv, T., Guihen, D., Kiriakoulakis, K., Lavaleye, M., and Duineveld, G.: A
884 Freiwald, JM Roberts, Cold-water coral ecosystem (Tisler Reef, Norwegian Shelf) may be a hotspot for
885 carbon cycling, *Marine Ecology Progress Series*, 465, 11-23, 2012.

886 Wienberg, C., and Titschack, J.: Framework-forming scleractinian cold-water corals through space and
887 time: a late Quaternary North Atlantic perspective, Ros-si S, Bramanti L, Gori A, Orejas C, *Marine Animal
888 Forests: the Ecology of Benthic Biodiversity Hotspots*, Springer, 699-732 pp., 2017.

889 Wienberg, C., Titschack, J., Freiwald, A., Frank, N., Lundälv, T., Taviani, M., Beuck, L., Schröder-Ritzrau,
890 A., Krengel, T., and Hebbeln, D.: The giant Mauritanian cold-water coral mound province: Oxygen control
891 on coral mound formation, *Quaternary Science Reviews*, 185, 135-152, 2018.

892 Wilson, J.: 'Patch' development of the deep-water coral *Lophelia pertusa* (L.) on Rockall Bank, *Journal of
893 the Marine Biological Association of the United Kingdom*, 59, 165-177, 1979.

894 Zabel, M., Boetius, A., Emeis, K.-C., Ferdelman, T. G., and Spieß, V.: PROSA Process Studies in the Eastern
895 South Atlantic – Cruise No. M76 – April 12 – August 24, 2008 – Cape Town (South Africa) – Walvis Bay
896 (Namibia). , DFG Senatskommission für Ozeanographie, METEOR-Berichte, M76, 180 pp., 2012.

897 11. Figure captions

898 **Figure 1** (a) Overview map showing the research areas off Angola and Namibia (red squares) and main features of the surface
899 water circulation (arrows) and frontal zone (dashed line) in the SE Atlantic as well as the two main rivers discharging at the
900 Angolan margin. Detailed bathymetry maps of the Angolan (upper maps) and Namibian margins (lower maps) showing the
901 position of (b) CTD transects (note the deep CTD cast down to 1000 m water depth conducted off Namibia) and (c) bottom
902 lander deployments (red squares shown in b indicate the cutouts displayed in c).

903 **Figure 2** ROV images (copyright MARUM ROV SQUID, Bremen, Germany) showing the surface coverage of cold-water coral
904 mounds discovered off Namibia (a, b) and Angola (c, d). Images were recorded and briefly described for their faunal
905 composition during RV *Meteor* cruise M122 "ANNA" (see Hebbeln et al. 2017). (a) Sylvester mound, 225 m water depth. Dead
906 coral framework entirely consisting of *L. pertusa*. The framework is intensely colonized by the yellow bryozoan *Metropriella* sp.,
907 zoanthids, actinarians and sponges. Vagile fauna consists of asteroids and gobiid fishes (*Sufflogobius bibarbatus*) that hide in
908 hollows in the coral framework. (b) Sylvester mound, 238 m water depth. Dense coral rubble (*L. pertusa*) heavily overgrown by
909 *Metropriella* sp. and sponges. Note the decapod crab *Macropipus australis* (center of the image). (c) Valentine mound, 238 m
910 water depth. Live *L. pertusa* colony being grazed by echinoids. Note the sponge *Aphrocallistes* sp. with its actinarian symbionts
911 (right side of the image). (d) Buffalo mound, 345 m water depth. Living CWC reef observed on top of an Angolan coral mound.
912 Many fishes are present around the reef (*Helicolenus dactylopterus*, *Gephyroberyx darwinii*).

913 **Figure 3** TS-diagrams showing the different water masses being present at the (a) Namibian and (b) Angolan margins: South
914 Atlantic Subtropical Surface Water (SASSW), South Atlantic Central Water (SACW) and Eastern South Atlantic Central water

915 (ESACW), Antarctic Intermediate Water (AAIW) (data plotted using Ocean Data View v.4.7.8; <http://odv.awi.de>; Schlitzer, 2011).
916 Red dotted line indicates the depth range of cold-water coral mound occurrence.

917 **Figure 4** CTD transect across the Namibian margin (see Fig. 1b for location). Data are presented for: (a) potential temperature
918 ($^{\circ}\text{C}$), (b) salinity (PSU), (c) dissolved oxygen concentrations (ml l^{-1}), note the pronounced oxygen minimum zone (OMZ) between
919 100-335 m water depth, and d) fluorescence (mg m^{-3}) (data plotted using Ocean Data View v.4.7.8; <http://odv.awi.de>; Schlitzer,
920 2011). The occurrence of fossil CWC mounds is indicated by a red dashed line, colored dots indicate bottom lander
921 deployments.

922 **Figure 5** CTD transect across the Angolan margin. Shown are data for (a) potential temperature ($^{\circ}\text{C}$), (b) salinity (PSU), (c)
923 dissolved oxygen concentration (ml l^{-1}), (d) fluorescence (mg m^{-3}), (e) turbidity (NTU) (data plotted using Ocean Data View
924 v.4.7.8; <http://odv.awi.de>; Schlitzer, 2011). The depth occurrence of CWC mounds is marked by a red, dashed line, the lander
925 deployments are indicated by colored dots.

926 **Figure 6** Data recorded by the ALBEX lander (210 m) at the Namibian margin in January 2016. Shown are data for temperature
927 ($^{\circ}\text{C}$; red), dissolved oxygen concentrations (ml l^{-1} ; blue), optical backscatter (turbidity; moss green), fluorescence (counts per
928 second green), current speed (m s^{-1} ; pink), current direction (degree: 0-360 $^{\circ}$; dark red) as well as nitrogen (mg l^{-1} ; pink dots),
929 carbon (mg l^{-1} ; purple dots), and chlorophyll- α concentration ($\mu\text{g l}^{-1}$; green dots) of SPOM collected during the first 48h by the
930 McLane pump. These data are supplemented by wind speed and direction (small black arrows) recorded concurrently to the
931 lander deployment by ship bound devices. Note that current directions changed from a generally south-poleward to an
932 equatorward direction when wind speed exceeded 10 m s^{-1} (stormy period indicated by black arrow).

933 **Figure 7** Lander data (ALBEX) recorded during the shallow (~ 340 m water depth) and deep deployments (~ 530 m water depth)
934 off Angola (January 2016). Shown are temperature ($^{\circ}\text{C}$; red), dissolved oxygen concentration (ml l^{-1} ; blue), fluorescence (counts
935 per second; green), optical backscatter (turbidity; yellow), current speed (m s^{-1} ; pink) and current direction (degree: 0-360 $^{\circ}$;
936 purple) as well as nitrogen (mg l^{-1} ; pink dots), carbon (mg l^{-1} ; purple dots), and chlorophyll- α concentration ($\mu\text{g l}^{-1}$; green dots) of
937 SPOM collected during the both deployments by the McLane pump.

938 **Figure 8** Composite records of SPOM collected by the McLane pump of the ALBEX lander at the Namibian and Angolan margins
939 during all three deployments. (a) $\delta^{15}\text{N}$ and $\delta^{13}\text{C}$ isotopic values at the Namibian (red dots) and Angolan (blue and green dots)
940 margins. Indicated by the square boxes are common isotopic values of terrestrial and marine organic matter (Boutton 1991,
941 Holmes et al. 1997, Sigman et al. 2009). The relative contribution of terrestrial material (green boxes) is increasing with a more
942 negative $\delta^{13}\text{C}$ value. (b) Total organic carbon (TOC) and nitrogen (N) concentration of the SPOM. Values of the Namibian
943 margin are marked by a blue circle (C/N ratio = 7.8), values of the Angolan margin are marked by a green circle (C/N ratio = 9.6).
944 Dissolved oxygen concentrations are included to show the higher nutrient concentrations in less oxygenated water.

945 **Figure 9** Depth range of cold-water coral mound occurrences (blue shaded areas) at the (a) Namibian and (b) Angolan margins
946 in relation to the dissolved oxygen concentrations and potential temperature. Diurnal tides are delivering mainly phytodetritus
947 (shown in (a) and organic matter from the benthic nepheloid layer (shown in (b) as well as oxygen from above, and from below
948 to the mound sites (indicated by blue arrows, the length of which indicate the tidal ranges).

949 **12. Tables**

950 **Table 1.** Metadata of lander deployments conducted during RV *Meteor* cruise M122 (ANNA) in January 2016. The deployment
 951 sites are shown in Figure 1.

	Station no. (GeoB ID)	Area	Lander	Date	Latitude [S]	Longitude [E]	Depth [m]	Duration [days]	Devices
Namibia	20507-1	on-mound	ALBEX	01.- 09.01.16	20°44.03'	12°49.23'	210	7.8	+ particle pump
	20506-1	off-mound	SLM	01.- 16.01.16	20°43.93'	12°49.11'	230	12.5	
Angola	20921-1	off-mound	ALBEX	20.- 23.01.16	9°46.16'	12°45.96'	340	2.5	+ particle pump
	20940-1	off-mound	ALBEX	23.- 26.01.16	9°43.84'	12°42.15'	530	2.6	+ particle pump
	20915-2	off-mound	SLM	19.- 26.01.16	9°43.87'	12°43.87'	430	6.8	

952

953 **Table 2** Environmental properties at the Namibian and Angolan margins.

	Namibia	Angola
Temperature [°C]	11.8-13.2	6.73-12.9
DO concentration [ml l ⁻¹]	0-0.15	0.5-1.5
Fluorescence [NTU]	42-45	38.5-41.5
Current speed max. [m s ⁻¹]	0.21	0.3
Current speed average [m s ⁻¹]	0.09	0.1
Tidal cycle	Semi-diurnal (0.37 dbar, 3 cm s ⁻¹)	Semi-diurnal (0.6 dbar, 8.2 cm s ⁻¹)
Average pH	8.01	8.12

954

955 **Table 3** Tidal analysis of the ALBEX lander from 6 m above the sea floor. Depth, mean current speed, mean current direction,
 956 tidal prediction of pressure fluctuations, two most important harmonics with amplitude, tidal prediction of horizontal current
 957 field, two most important harmonics with semi-major axis' amplitude.

	Station no. (GeoB ID)	Depth (m)	Mean current speed (cm s ⁻¹)	Current direction (°)	Tides [%] (p)	Const. [dbar]	Tides [%] (u)	Const. [cm s ⁻¹]
Namibia	20507-1	430	9.34	221.6	81.8	M2: 0.37	10.5	M2: 3.1 M3: 0.8
Angola	20921-1	340	9.96	247.9	91.6	M2: 0.59 M3: 0.04	36	M2: 7.8 M8: 0.7
	20940-1	530	8.92	275.6	86.8	M2: 0.60 M8: 0.02	50.9	M2: 8.6 M3: 3.7

958

